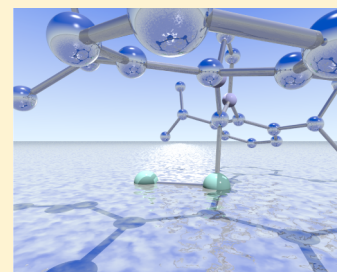


## N-Heterocyclic Carbene—Main-Group Chemistry: A Rapidly Evolving Field

Yuzhong Wang and Gregory H. Robinson\*

Department of Chemistry, The University of Georgia, Athens, Georgia 30602-2556, United States

**ABSTRACT:** This Award Article targets the evolving, yet surprisingly fruitful, chemistry of N-heterocyclic carbenes with low-oxidation-state main-group elements. Specifically, the chemistry of carbene-stabilized diatomic allotropes, diborenes, gallium octahedra, beryllium borohydride, and a host of related compounds will be presented. Providing a valuable historical perspective, the foundational work concerning the organometallic chemistry of gallium with sterically demanding *m*-terphenyl ligands from this laboratory will also be discussed.



## INTRODUCTION

Greek philosophers pondered fundamental issues of matter and composition centuries before alchemists began practicing their elusive arts. Believing all change was a consequence of attraction and repulsion, Empedocles proposed four indestructible and unchangeable terrestrial elements: Earth, Air, Fire, and Water.<sup>1</sup> The popularity of this “elemental theory” sufficiently increased such that other philosophers, most notably Plato and Aristotle, embraced it. Indeed, in addition to the four terrestrial elements originally proposed by Empedocles, Aristotle proposed a lone celestial element: *Aether*. Perhaps driven by convenience, and possibly a portent of the modern practice of chemistry, Platonic solids were ultimately taken as “symbols” for these elements: Cube (Earth), Octahedron (Air), Tetrahedron (Fire), Icosahedron (Water), and Dodecahedron (*Aether*) (Figure 1).

While it is unlikely that Empedocles, Plato, or Aristotle seriously influenced the development of chemistry as a legitimate science, it is intriguing to frame their views alongside those of Dmitri Mendeleev and Lothar Meyer when one gazes upon the Periodic Table of Elements.

From the quest of the chemist to synthesize new molecules to the fabrication of advanced electronic devices or the search for alternative energy sources, the modern practice of chemistry is as wide as it is varied. Yet the wonder, power, and magic of chemistry is often glimpsed on a more fundamental level: when one holds a (surprisingly heavy) flask of mercury, uses a candle to ignite a (small) hydrogen balloon, or drops (small) pieces of potassium into water. Such experiences with the actual elements often elicit an emotional—possibly even an “elemental”—response in individuals. The fascination of chemistry is further enhanced by the concept of allotropy: How is it possible that two forms of the same element can have such disparate chemical and physical properties?

This Award Article, portions of which were presented in the lecture of the F. Albert Cotton Award in Synthetic Inorganic Chemistry at the 253rd National Meeting of the American

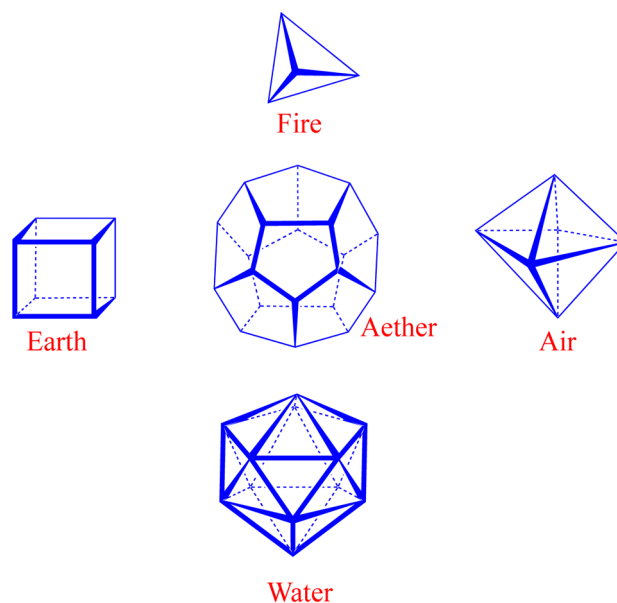


Figure 1. Elements of Empedocles, Plato, and Aristotle.

Chemical Society (New Orleans, April 2013), targets the evolving, yet surprisingly fruitful, low-oxidation state main-group chemistry of N-heterocyclic carbenes. A particular emphasis is placed on the stabilization of highly reactive main-group diatomic allotropes. In an effort to provide historical context, this Award Article begins with the foundational work that preceded our recent research in main-group chemistry of NHCs:<sup>2–4</sup> the low-oxidation-state gallium chemistry involving sterically demanding *m*-terphenyl ligands.<sup>5</sup>

Received: September 12, 2014

Published: October 24, 2014



## METALLOAROMATICITY AND Ga–Ga TRIPLE BONDS

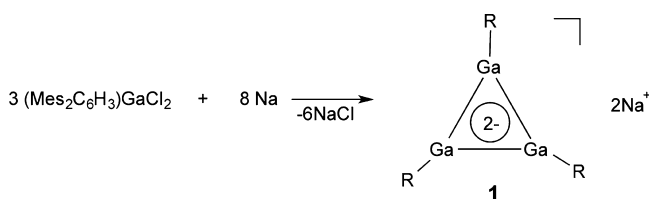
While the concept has long since evolved beyond its original, if dubious, association with fragrance, aromaticity remains one of the most prominent cornerstones of chemistry.<sup>6</sup> Presently, aromaticity spans compounds ranging from the classic aromatics, which generally possess planar hydrocarbon rings with  $(4n + 2)$   $\pi$  electrons, to diverse heterocycles and even three-dimensional molecular systems.<sup>7,8</sup> Notably, aromaticity has stubbornly remained a steadfast beacon between organic chemistry and inorganic chemistry. Borazine—the  $B_3N_3$  six-membered ring compound prepared by Alfred Stock in 1926<sup>9</sup>—was ultimately, if inaccurately, proffered as “inorganic benzene”. Arguably, the most enduring aspect of borazine may be that it allowed inorganic chemists to confidently venture into “the aromatic realm”.

Although benzene and borazine share a number of similar physical properties, their chemical behavior is quite disparate. Most prominently, benzene readily undergoes electrophilic aromatic substitution reactions and produces substitution products. In contrast, borazine exclusively yields addition products from the same systems. Thus, it has become increasingly difficult to make a compelling argument for significant aromatic character in borazine. While benzene-based six-membered rings are the most prominent class of aromatic molecules, it is interesting to note that smaller carbon ring systems may also display aromatic behavior. Indeed, Breslow’s preparation of the triphenylcyclopropenium cation, the smallest aromatic ring system, remains a milestone.<sup>10</sup> This laboratory pondered a compelling question in the mid-1990s: Might molecules containing metallic ring systems display traditional aromatic behavior?

To this end, a significant portion of our early work concerned the organogallium chemistry of sterically demanding *m*-terphenyl ligands.<sup>5</sup> The utilization of the 2,6-dimesitylphenyllithium reagent proved critical in this work.<sup>11,12</sup> Reaction of 2,6-dimesitylphenyllithium,  $(Mes_2C_6H_3)Li$ , with gallium chloride in a molar ratio of 2:1 gave bis(2,6-dimesitylphenyl)gallium chloride,  $(Mes_2C_6H_3)_2GaCl$ , in modest yield.<sup>13</sup> Our alkali-metal reduction attempts of  $(Mes_2C_6H_3)_2GaCl$  were frustratingly unsuccessful. The steric bulk of the two *m*-terphenyl ligands around the central gallium atom may have simply been too large for the meaningful approach of two gallium atoms to sustain sufficient orbital overlap.

Consequently, we pursued this project with 2,6-dimesitylphenylgallium dichloride,  $(Mes_2C_6H_3)GaCl_2$ . Reaction of finely divided sodium metal with  $(Mes_2C_6H_3)GaCl_2$  produced a dark-red solution that ultimately yielded  $Na_2[(Mes_2C_6H_3)Ga]_3$  (**1**) as extremely air-sensitive dark-red crystals (Scheme 1;  $R = Mes_2C_6H_3$ ).<sup>14</sup> Notably, compound **1** represents the first organometallic compound containing an aromatic gallium ring: the first *cyclogallene*.<sup>15</sup>

### Scheme 1. Synthesis of **1**



Compound **1** possessed an inherently planar three-membered  $Ga_3$  ring with  $Ga-Ga-Ga$  bond angles of  $60.0(1)^\circ$  (Figure 2).<sup>14</sup> On either side of the  $Ga_3$  ring resided

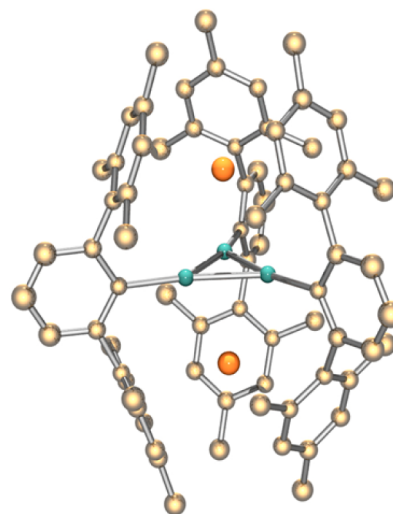


Figure 2. Molecular structure of **1**.

a sodium atom [ $Ga \cdots Na = 3.229(2)$  Å]. The  $Ga-Ga$  bond distance of  $2.441(1)$  Å in **1** was among the shortest reported,<sup>5</sup> which is consistent with the fact that each of the two sodium atoms contributes one electron to the empty  $p$  orbitals of the three  $sp^2$ -hybridized gallium atoms, thus providing the two delocalized  $\pi$  electrons necessary for aromaticity.

Moreover, the delocalized  $\pi$  cloud of the  $Na_2[GaH]_3$  model compares well to that of the aromatic cyclopropenium model ( $[CH]_3^+$ ) (Figure 3).<sup>16</sup> It should be noted, however, that the

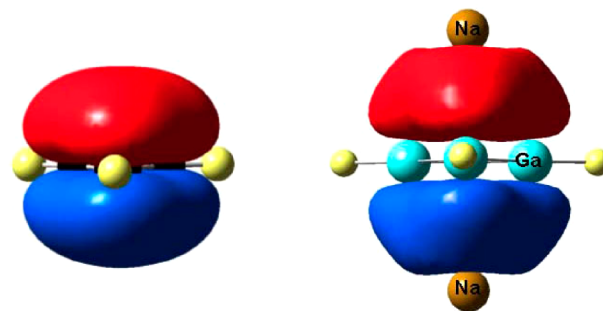


Figure 3. Delocalized  $\pi$  orbitals of  $[CH]_3^+$  and  $Na_2[GaH]_3$  models.

neutral model  $[GaH]_3$  was predicted to be unstable.<sup>16</sup> Indeed, the neutral analogue of **1** has not been isolated. Consequently, we deemed it appropriate to employ the term *metalloaromaticity*<sup>17</sup> to describe **1** and subsequently reported gallium rings such as  $K_2[Ga_4R_2]$  [ $R = C_6H_3-2,6-(C_6H_2-2,4,6-Pr^i)_2$ ]<sup>18</sup> and  $Na_2[Ga_4R_4](THF)_2$  [ $R = Si(Bu^i)_3$ ],<sup>19</sup> wherein traditional aromatic behavior is exhibited by metallic ring systems instead of cyclic hydrocarbons.<sup>15</sup> These discoveries thus suggest that other ionic organic molecules and concepts may also be experimentally realized from an inorganic perspective.

Because aromaticity is related to induced ring currents, we explored the metalloaromaticity of **1** by computing the nucleus independent chemical shift (NICS)<sup>6</sup> values of  $M_2[GaH]_3$  ( $M = Li, Na, \text{ and } K$ ) models.<sup>16</sup> As a standard, the NICS value for benzene was taken as  $-11.5$ . Correspondingly, the NICS values

for the lithium, sodium, and potassium model systems [i.e.,  $\text{Li}_2[\text{GaH}]_3$ ,  $\text{Na}_2[\text{GaH}]_3$ , and  $\text{K}_2[\text{GaH}]_3$ ] were shown to be  $-13.0$ ,  $-15.0$ , and  $-15.0$ , respectively, indicating the aromatic character of these species.

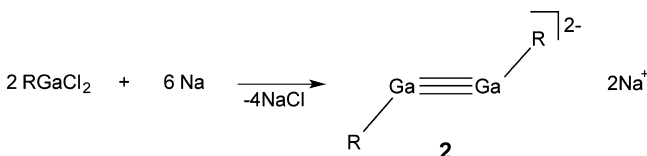
This laboratory subsequently prepared the potassium cyclogallene analogue,  $\text{K}_2[(\text{Mes}_2\text{C}_6\text{H}_3)\text{Ga}]_3$ , which exhibits structural parameters similar to those of **1**.<sup>20</sup> More than a decade after the report of **1**, Power et al.<sup>21</sup> prepared the aluminum analogue, a metalloaromatic cycloaluminene  $\text{Na}_2[(\text{Mes}_2\text{C}_6\text{H}_3)\text{Al}]_3$ .

*"How Short is a Gallium–Gallium Triple Bond?"*

It has been nearly two decades since this cryptic question was naively posited in the title of a brief report from this laboratory. This report concerned the synthesis and molecular structure of a highly unusual molecule that was described as the first digallyne: the first compound containing a Ga–Ga triple bond.<sup>22</sup> The answer to this question has proven to be considerably less important than the fundamental issues that were immediately raised in vigorous debates concerning this compound (*vide infra*).

That small electronic and steric adjustments of a given ligand can have a substantial impact on the character of the metal center is a fundamental tenet of chemistry. Having prepared the first metalloaromatic cyclogallenes, we were interested in exploring the organogallium chemistry based on even larger *m*-terphenyl ligands such as the 2,6-bis(2,4,6-triisopropylphenyl)phenyl ligand. The first step was to install this ligand onto a gallium center. Reaction of the lithium derivative of this *m*-terphenyl ligand with gallium chloride afforded dimeric  $\text{RGaCl}_2$  [ $\text{R} = \text{C}_6\text{H}_3\text{-}2,6\text{-}(\text{C}_6\text{H}_2\text{-}2,4,6\text{-}\text{Pr}^i)_2$ ],<sup>23</sup> which was then reduced by sodium metal (in diethyl ether) gave  $\text{Na}_2[\text{RGa}\equiv\text{GaR}]$  (**2**) as red crystals (Scheme 2).<sup>22</sup>

**Scheme 2. Synthesis of 2**



Similar to **1**, the two sodium cations perch on either side of the  $\text{Ga}_2$  core of **2** ( $\text{Ga}\cdots\text{Na} = 3.08 \text{ \AA}$ , *av*; Figure 4).<sup>22</sup> Two bulky *m*-terphenyl ligands provide effective steric shielding of the almost planar four-membered  $\text{Ga}_2\text{Na}_2$  ring. The most

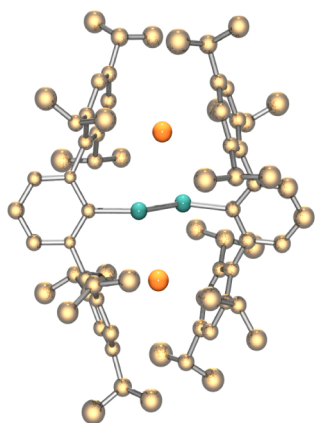


**Figure 4.** Molecular structure of **2**.

remarkable structural features of **2** include the following: (1) The Ga–Ga bond distance of  $2.319(3) \text{ \AA}$ , which is among the shortest reported. Moreover, Pyykkö et al. in an article entitled “Triple-Bond Covalent Radii” concluded that “With respect to the  $\text{Ga}\equiv\text{Ga}$  triple bond suggested by Robinson’s group, our results do not disagree with the idea. In fact, their homonuclear Ga–Ga bond distance of  $232 \text{ pm}$  [ $2.32 \text{ \AA}$ ] is shorter than twice the present  $r(\text{Ga})$  value of  $121 \text{ pm}$  [ $1.21 \text{ \AA}$ ], largely based on heteronuclear pairs.”<sup>24</sup>; (2) The nonlinear (or trans-bent) geometry around the Ga–Ga bond with an average C–Ga–Ga bond angle of  $131.0^\circ$ . Our claim of compound **2** as the first example of a Ga–Ga triple bond, the first *digallyne*,<sup>22</sup> initiated a lively debate concerning the fundamental issues of structure and bonding of this unusual molecule.<sup>24–36</sup>

When engaging in element–element multiple bonding, the heavier main-group elements often behave in a fashion much different from that observed for carbon. For instance, similar to digallyne **2**, Sekiguchi’s disilyne<sup>37</sup> also possesses a trans-bent geometry about the Si–Si triple bond with a  $\text{Si}\equiv\text{Si}-\text{Si}$  bond angle of  $137.44^\circ$ , which is very close to the average Ga–Ga–C bond angle ( $131.0^\circ$ ) of **2**.<sup>22</sup> According to our density functional theory (DFT) computations, the trans-bent character of the Ga–Ga triple bond in **2** may be ascribed to the formation of two donor–acceptor (dative) bonds and one  $\pi$  bond (populated by two electrons from the two sodium atoms) between two gallium atoms in **2** (Figure 5).<sup>25,26</sup> The 2.794 NLMO/NPA bond order of the Ga–Ga bond in the **2-Ph** model (i.e.,  $\text{Na}_2[\text{RGaGaR}]$ ,  $\text{R} = 2,6\text{-Ph}_2\text{C}_6\text{H}_3$ ) supports the digallyne formulation of **2**.<sup>26</sup>

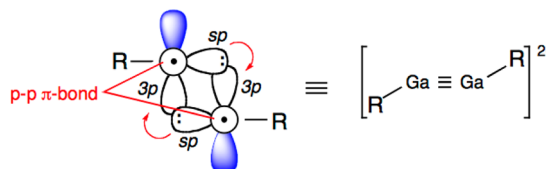


**Figure 5.** Proposed bonding mode of **2**.

Power et al.<sup>21</sup> ultimately prepared a dialuminyne,  $\text{Na}_2[\text{RAL-AIR}]$  [ $\text{R} = \text{C}_6\text{H}_3\text{-}2,6\text{-}(\text{C}_6\text{H}_3\text{-}2,6\text{-}\text{Pr}^i)_2$ ], the long sought aluminum analogue of the digallyne **2**, by the sodium reduction of the corresponding  $\text{RALI}_2$  precursor. The  $2.428(1) \text{ \AA}$  Al–Al bond distance in this dialuminyne compound was found to be ca.  $0.23 \text{ \AA}$  shorter than that for the reported Al–Al single bond in  $\text{R}_2\text{Al-AIR}_2$  [ $\text{R} = \text{CH}(\text{SiMe}_3)_2$ ] [ $2.660(3) \text{ \AA}$ ].<sup>38</sup> The coordination geometry around the Al–Al bond in  $\text{Na}_2[\text{RAL-AIR}]$  was also shown to be trans-bent with a Al–Al–C bond angle of  $131.71(7)^\circ$ —closely approached the average Ga–Ga–C angle of  $131.0^\circ$  for **2**.<sup>22</sup>

DFT computations suggested that the dialuminyne model (i.e.,  $\text{Na}_2[\text{RAL-AIR}]$ ,  $\text{R} = 2,6\text{-Ph}_2\text{C}_6\text{H}_3$ ) contains one out-of-plane  $\pi$  bond (highest occupied molecular orbital, HOMO), a slipped  $\pi$  bond (HOMO–1), and a  $\sigma$  bond (HOMO–2).<sup>21</sup> Significantly, this bonding description for the dialuminyne molecule is very similar to that of **2** proposed by Bytheway and Lin: “The Ga–Ga bonding in trans-bent  $[\text{Ga}_2\text{R}_2]^{2-}$  molecules is thus better described as having a distorted  $\sigma$ -bond, a significantly weakened  $\pi$ -bond which is localized strongly on the gallium atoms, and a pure  $\pi$ -bond perpendicular to the  $\text{Ga}_2\text{C}_2$  plane.”<sup>31</sup> The Wiberg bond indices (WBIs) of **2-Ph** ( $2.02$ )<sup>26</sup> and Power’s dialuminyne ( $1.13$ )<sup>21</sup> are obviously lower than their formal bond order of 3.0. However, it is noteworthy

that for many cases the WBI values are smaller than the corresponding formal bond order values. For example, the WBI value of the H–F bond in diatomic hydrogen fluoride is 0.67, and that of the B–N bond in  $\text{H}_3\text{B}-\text{NH}_3$  is only 0.55.<sup>26</sup>

Since we reported the cyclogallene (**1**) and digallyne (**2**), a number of interesting *m*-terphenyl-based main-group molecules with unusual structures and bonding motifs have been reported.<sup>39</sup> In an effort to explore the more subtle aspects of low-oxidation-state main-group chemistry, we ultimately moved beyond the formally anionic *m*-terphenyl ligands and began to focus on neutral NHCs. Perhaps this would provide an avenue to stabilize novel, highly reactive main-group species. The following sections document our progress in this area. Indeed, our interest in the main-group chemistry of NHCs may be traced to the synthesis of  $\text{L:M}(\text{CH}_3)_3$  [ $\text{L}: = \text{:C}\{(\text{Pr}^i)\text{NC}(\text{Me})\}_2$ ;  $\text{M} = \text{Al}$  and  $\text{Ga}$ ] nearly two decades ago.<sup>40</sup>

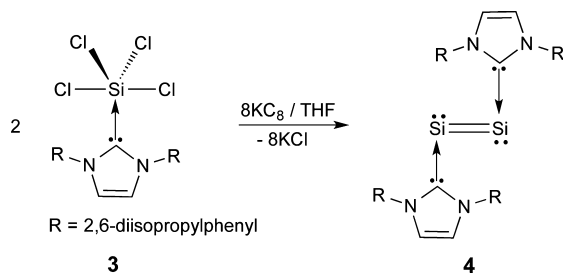
### ■ NHCS AND MAIN-GROUP DIATOMIC MOLECULES

The Periodic Table boasts only seven elements—hydrogen, nitrogen, oxygen, fluorine, chlorine, bromine, and iodine—that unambiguously exist as stable homonuclear diatomic molecules. Of these, the three lightest—hydrogen, oxygen, and nitrogen—are not only biologically relevant but also critical in a number of essential industrial chemical transformations. Thus, the activation of stable diatomic  $\text{H}_2$ ,  $\text{N}_2$ , and  $\text{O}_2$  molecules represents a fundamental strategy to utilize the chemical energy reserved in these simple molecules in building more complex molecular systems.<sup>41</sup> It should be noted that there are also highly reactive diatomic main-group molecules, such as  $\text{Si}_2$ ,  $\text{P}_2$ , and  $\text{As}_2$ , that typically are detectable as gaseous species at very high temperatures<sup>42–44</sup> or studied with matrix isolation techniques.<sup>45</sup> In order to probe their possibly fascinating, but largely unexplored, chemistry, this laboratory pioneered a *carbene stabilization strategy*.

The main-group chemistry of carbenes has experienced impressive growth over the past two decades.<sup>2–4,46–57</sup> The carbene ligands employed in our projects are sterically demanding NHCs [ $\text{L}: = \text{:C}\{\text{N}(2,6\text{-Pr}^i_2\text{C}_6\text{H}_3)\text{CH}\}_2$ ;  $\text{L}': = \text{:C}\{\text{N}(2,4,6\text{-Me}_3\text{C}_6\text{H}_2)\text{CH}\}_2$ ;  $\text{L}'': = \text{:C}\{(\text{Pr}^i)\text{NC}(\text{Me})\}_2$ ]. These NHCs not only are relatively robust themselves but also may provide sufficient kinetic stability to target highly reactive main-group cores. In 2008, this laboratory reported the carbene complex  $\text{L:SiCl}_4$  [ $\text{L}: = \text{:C}\{\text{N}(2,6\text{-Pr}^i_2\text{C}_6\text{H}_3)\text{CH}\}_2$ ] adduct (**3**) by combining the carbene ( $\text{L:}$ ) with  $\text{SiCl}_4$ .<sup>58</sup> Potassium graphite reduction of **3** (1:4) in tetrahydrofuran (THF), afforded the carbene-stabilized disilicon  $\text{L:Si}=\text{Si:L}$  (**4**) as dark-red crystals (Scheme 3).<sup>58</sup>

Alternatively, allowing **3** to react with potassium graphite in a molar ratio of 1:6 in hexane afforded both **4** and the partially reduced bis-silylene intermediate  $\text{L:Si}(\text{Cl})-(\text{Cl})\text{Si:L}$  (**5**).<sup>58</sup>

#### Scheme 3. Synthesis of **4**



Roesky et al. subsequently synthesized another stable reduction intermediate,  $\text{L:SiCl}_2$ , by potassium graphite reduction of **3** in a 1:2 molar ratio.<sup>59</sup> The synthesis of disiladibene  $(\text{CAAC})_2\text{Si}_2$ , the CAAC-based analogue of **4** [ $\text{CAAC}^{60} = \text{cyclic alkyl(amine)carbene}$ ], was recently achieved (in 54% yield) by Roesky et al. via potassium graphite reduction of  $\text{CAAC:SiCl}_4$  (1:4 molar ratio).<sup>61</sup> As predicted by Bertrand et al.,<sup>51</sup> cyclic voltammetry investigation suggests that  $(\text{CAAC})_2\text{Si}_2$  can undergo one-electron reduction to form a highly reactive radical-anion intermediate. Moreover, one-electron-mediated rearrangement of  $(\text{CAAC})_2\text{Si}_2$  was also observed.<sup>61</sup>

The choice of the reducing agent plays a pivotal role in the synthesis of carbene-stabilized group 14 diatomic molecules,  $\text{L:E}=\text{E:L}$  ( $\text{L}: = \text{NHC}$ ;  $\text{E} = \text{group 14 elements}$ ). Potassium graphite is an effective reducing agent for the formation of **4**<sup>58</sup> but fails to yield  $\text{L:E}=\text{E:L}$  ( $\text{E} = \text{Ge}$  and  $\text{Sn}$ ) analogues of **4** through reduction of the corresponding  $\text{L:ECl}_2$  precursors. Jones and Frenking prepared both  $\text{L:Ge}=\text{Ge:L}$  (20% yield)<sup>62</sup> and  $\text{L:Sn}=\text{Sn:L}$  (5% yield)<sup>63</sup> [ $\text{L}: = \text{:C}\{\text{N}(2,6\text{-Pr}^i_2\text{C}_6\text{H}_3)\text{CH}\}_2$ ], using the unique compound  $\text{RMg}^1\text{-Mg}^1\text{R}$ <sup>64</sup> ( $\text{R} = [(\text{MesNC-Me})_2\text{CH}]$ ) as the reducing agent. The dramatically low yield of  $\text{L:Sn}=\text{Sn:L}$  [ $\text{L}: = \text{:C}\{\text{N}(2,6\text{-Pr}^i_2\text{C}_6\text{H}_3)\text{CH}\}_2$ ] suggests an increased challenge in stabilizing heavier analogues of **4**. Indeed, isolation of carbene-stabilized  $\text{Pb}_2$  has yet to be achieved. As the lightest homologue of  $\text{L:E}=\text{E:L}$  ( $\text{L}: = \text{NHC}$ ;  $\text{E} = \text{group 14 elements}$ ), carbene-stabilized  $\text{C}_2$  (i.e., a  $\text{C}_4$  cumulene) has been theoretically evaluated by Dutton and Wilson<sup>65</sup> and independently synthesized by both Roesky et al.<sup>66</sup> and Bertrand et al.<sup>67</sup> using CAAC scaffolds.

Compound **4** may be regarded as a dimer of the carbene-stabilized silicon atom ( $\text{L:Si}$ ) involving a  $\text{Si}=\text{Si}$  double bond (Figure 6). The  $\text{Si}=\text{Si}$  double-bond distance of **4** [2.2294(11)

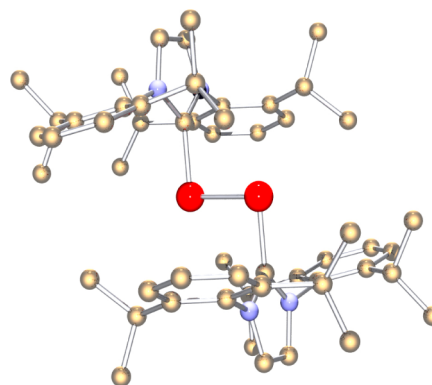


Figure 6. Molecular structure of **4**.

Å] not only is very similar to the experimental bond distance of  $\text{Si}_2$  (2.246 Å)<sup>68</sup> but also fits nicely in the range of reported disilene bond distances (2.14–2.29 Å).<sup>69</sup> This  $\text{Si}=\text{Si}$  double-bond distance, however, is about 0.08 Å shorter than the computed value for  $\text{OC:Si}=\text{Si:CO}$  (2.310 Å).<sup>70</sup> The  $\text{Si}=\text{Si}$  double-bond feature of **4** was further characterized by computations and spectral methods. The 1.73 WBI of the  $\text{Si}-\text{Si}$  bond in **4** is supportive of double-bond character. The HOMO and HOMO–1 of model **4-Ph** correspond to the  $\text{Si}-\text{Si}$   $\pi$  and  $\sigma$  bonds, respectively (Figure 7).<sup>58</sup> The  $\pi_{\text{Si}=\text{Si}}-\pi_{\text{Si}=\text{Si}}^*$  absorption ( $\lambda_{\text{max}} = 468$  nm, in THF) of **4** is comparable to the reported UV absorption maxima (390–480 nm) of disilenes.<sup>69</sup> The  $^{29}\text{Si}$  NMR resonance of **4** (224.5 ppm) is shifted downfield with respect to those (50–155 ppm) of disilenes.<sup>69</sup> The  $\text{Si}-\text{C}$

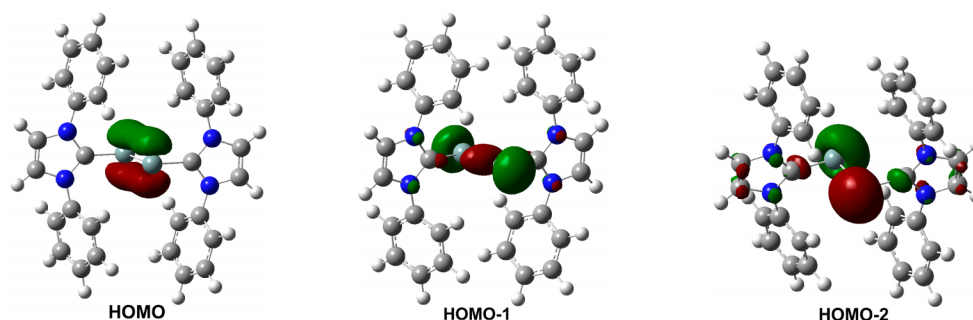


Figure 7. HOMO, HOMO-1, and HOMO-2 molecular orbitals of 4-Ph.

bond distance of **4** [1.9271(15) Å] compares well to those for **3** [1.928(2) Å] and other donor–acceptor types of Si–C bonds in **11–13** [1.917(3)–1.944(4) Å]<sup>71,72</sup> but is obviously shorter than that [2.000(2) Å] in a 1,3-disila-2-oxallyl zwitterion.<sup>73</sup> One of the most important structural features of **4** is its trans-bent geometry around the two-coordinate silicon atoms [C–Si–Si angle = 93.57 (11)°], which is in accordance with the presence of one lone pair of electrons at each silicon atom and a weak hybridization between 3s and 3p orbitals of silicon atoms in **4**. Natural bond orbital (NBO) analysis shows that the Si–Si  $\sigma$  bond has 82.2% p character and the Si–Si  $\pi$  bond has 99.6% p character, whereas the silicon lone-pair orbitals (such as HOMO-2 in Figure 2) have mainly s character (72.8% s character).<sup>58</sup>

Both the trans-bent geometry around the Si<sub>2</sub> core and the Si–C single bonds support that the silicon atoms in **4** are in the formal oxidation state of zero because the silicon(II) atoms would result in a linear C–Si–Si–C backbone with short Si=C double bonds.<sup>74</sup> In contrast to the triplet ground state ( $X^3\Sigma_g^-$ ) for the isolated Si<sub>2</sub> species,<sup>75</sup> **4** contains a singlet Si<sub>2</sub> core.

Because CAACs are more nucleophilic and electrophilic than NHCs,<sup>60</sup> it is interesting to compare the structural parameters between **4** and (CAAC)<sub>2</sub>Si<sub>2</sub>.<sup>61</sup> Like **4**, the noncentral symmetric (CAAC)<sub>2</sub>Si<sub>2</sub> also adopts a trans-bent geometry around the Si<sub>2</sub> unit. The C–Si–Si angles [103.18(13)°, av] are about 10° larger than that for **4** [93.57(11)°]. Both the Si=Si double bond distance [2.254(3) Å] and the <sup>29</sup>Si NMR chemical shift (249.1 ppm) of (CAAC)<sub>2</sub>Si<sub>2</sub> compares well to those of **4** [ $d_{\text{Si=Si}} = 2.2294(11)$  Å;  $\delta$  (<sup>29</sup>Si NMR) = 224.5 ppm]. However, the Si–C bond of (CAAC)<sub>2</sub>Si<sub>2</sub> [1.887(4) Å] is shorter than that in **4** [1.9271(15) Å], but longer than the typical Si=C double bonds (1.702–1.775 Å).<sup>76</sup> While the imidazole rings in **4** are almost perpendicular to the Si=Si core, the five-membered C<sub>4</sub>N rings in (CAAC)<sub>2</sub>Si<sub>2</sub> are somewhat coplanar to the Si<sub>2</sub> unit. All of these structural changes of (CAAC)<sub>2</sub>Si<sub>2</sub> with respect to **4** suggest that the Si–C bond of (CAAC)<sub>2</sub>Si<sub>2</sub> has partial double-bond character, in which the silicon atoms not only accept the  $\sigma$ -donated electron pairs from the CAAC ligands but also  $\pi$ -back-donate electron pairs to the empty p orbitals of the carbene carbon atoms.<sup>61</sup>

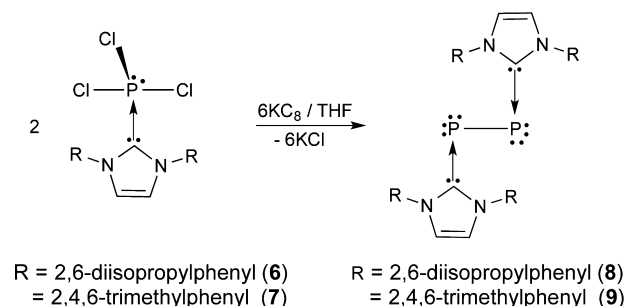
The heavier analogues of **4**, L:E=E:L [E = Ge and Sn; L = :C{N(2,6-Pr<sup>i</sup><sub>2</sub>C<sub>6</sub>H<sub>3</sub>)CH}<sub>2</sub>], are isostructural to **4**, adopting a trans-bent geometry around the E<sub>2</sub> cores [C–Ge–Ge angle = 89.87(8)°;<sup>62</sup> C–Sn–Sn angle = 91.82(8)°].<sup>63</sup> In contrast, both theoretical and experimental results suggest that the carbene-stabilized dicarbon has an almost linear C<sub>4</sub> cumulene structure [C<sub>carbene</sub>–C–C angle = 178.82(15)°; C<sub>carbene</sub>–C bond distance = 1.3236(16) Å; C–C bond distance = 1.249(2) Å], which may

undergo one- and two-electron oxidation to form the corresponding radical-cation and dication derivatives, respectively.<sup>65–67</sup>

In contrast to ubiquitous and extraordinarily stable dinitrogen (N<sub>2</sub>), the heavier group 15 diatomic congeners, such as P<sub>2</sub> and As<sub>2</sub>, are transient molecules and generally detectable at high temperatures. Metastable white phosphorus (P<sub>4</sub>) activation is an effective means to access transition metal–diphosphorus complexes.<sup>77,78</sup> A niobium diphosphaazide-based mild thermal transfer of P<sub>2</sub> to the organic substrate is also noteworthy.<sup>79–81</sup> In transition-metal complexes of P<sub>2</sub>, P<sub>2</sub> may behave as a four-, six-, or eight-electron donor.<sup>42</sup> Utilizing this carbene-stabilization strategy, we isolated the first carbene-stabilized P<sub>2</sub> complexes (**8** and **9**), in which P<sub>2</sub> behaves as a Lewis acid for the first time.<sup>82</sup>

NHC-stabilized P<sub>2</sub> complexes (**8** and **9**) were synthesized by potassium graphite reduction of the corresponding PCl<sub>3</sub> precursors [i.e., L:PCl<sub>3</sub>, where L = :C{N(2,6-Pr<sup>i</sup><sub>2</sub>C<sub>6</sub>H<sub>3</sub>)CH}<sub>2</sub> (**6**); L':PCl<sub>3</sub>, where L' = :C{N(2,4,6-Me<sub>3</sub>C<sub>6</sub>H<sub>2</sub>)CH}<sub>2</sub> (**7**); Scheme 4].<sup>82</sup> Both of these compounds were isolated as air-

#### Scheme 4. Synthesis of **8** and **9**



sensitive red crystals. However, the yield of **8** (57%) was much higher than that of **9** (21%), perhaps indicating the importance of the steric bulk of the carbenes in stabilization of the reactive P<sub>2</sub> core. Notably, carbene-based P<sub>4</sub> activation has been actively utilized in the synthesis of a series of carbene-stabilized P<sub>n</sub> (n = 1, 2, 4, and 12) complexes.<sup>83–85</sup>

The central P–P bonds in **8** [2.2052(10) Å] and **9** [2.1897(11) Å] compare well to the P–P single bonds in P<sub>4</sub> (2.21 Å).<sup>42</sup> The single-bond essence is further supported by the 1.004 P–P WBI of the simplified model.<sup>82</sup> Thus, the increase in steric bulk of the carbenes may remarkably affect the conformations of carbene-stabilized P<sub>2</sub> complexes. Indeed, with the increase of the steric bulk of the carbenes, the C–P–P–C torsion angle correspondingly increases from the computed value of 98.6° in the simplified model L:P–P:L [L:

= :C(NHCH)<sub>2</sub>, optimized in C<sub>2</sub> minimum symmetry] to 134.1° for **9** (in a gauche conformation) and finally to 180.0° for **8** (in C<sub>i</sub> symmetry), adopting a trans-bent geometry (Figure 8).<sup>82</sup>

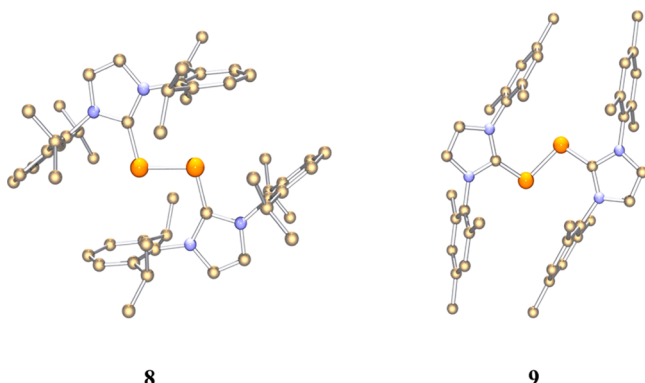


Figure 8. Molecular structures of **8** and **9**.

The phosphorus atoms in **8** and **9** are two-coordinate and have a bent geometry with C–P–P bond angles of 103.2° and 102.6°, respectively. The localized molecular orbital (LMO) study on the model L:P–P:L [L: = :C(NHCH)<sub>2</sub>, optimized in C<sub>2h</sub> symmetry] shows that each phosphorus atom bears two lone-pair orbitals. According to NBO analysis, one is predominantly s character (68.8% s, 31.2% p, and 0.0% d), and the other is essentially pure p (0.0% s, 99.8% p, and 0.2% d). Consequently, the latter may back-donate electrons to the vacant p orbital of the carbene carbon atom, rendering a 1.397 WBI of the P–C<sub>NHC</sub> bond that bears modest double-bond character. The X-ray structural parameters of **8** and **9** support this bonding description. For instance, the imidazole ring is almost coplanar with the P<sub>2</sub> core [the N(2)–C(1)–P(1)–P(1A) torsion angle = 2.3° for **8** and 8.2° (av) for **9**]. The P–C<sub>NHC</sub> bond distance of 1.7504(17) Å is between P=C double bond distances (1.65–1.67 Å) of the nonconjugated phosphalkenes<sup>86</sup> and typical P–C single bond distances [1.871(11) Å P–C bond distance for **6**].<sup>87</sup> CAAC-stabilized P<sub>2</sub> exhibits a relatively short P–C bond distance of 1.719(7) Å, which, coupled with its low-field <sup>31</sup>P chemical shift (54.2 ppm), suggests that the CAAC–P<sub>2</sub> complex has a 2,3-diphosphabutadiene structure.<sup>85</sup> In contrast, both the high-field <sup>31</sup>P chemical shifts for **8** (–52.4 ppm) and **9** (–73.6 ppm) and the approximate 1.75 Å P–C bond distances support the presence of electron-rich bis(phosphinidene) cores in these two molecules.<sup>82</sup>

Parallel to the synthetic route of **8** (Scheme 4), reaction of AsCl<sub>3</sub> with the carbene ligand (L:) at ambient temperature gives hypervalent L:AsCl<sub>3</sub> [L: = :C{N(2,6-Pr<sup>i</sup><sub>2</sub>C<sub>6</sub>H<sub>3</sub>)CH}<sub>2</sub>] in almost quantitative yield, which is then reduced by potassium graphite in THF to afford L:As–As:L (**10**) as air-sensitive red crystals in 19% yield.<sup>88</sup> When the less bulky L': carbene [L': = :C{N(2,4,6-Me<sub>3</sub>C<sub>6</sub>H<sub>2</sub>)CH}<sub>2</sub>] was employed, isolation of the corresponding carbene–As<sub>2</sub> complex did not succeed.

The As–As bond of **10** [2.442(1) Å] (Figure 9) is a typical As–As single bond with 91% As 4p character [WBI = 1.009, based on the simplified model L:As–As:L, L: = :C(NHCH)<sub>2</sub>, **10-H**], which compares well to that for gaseous As<sub>4</sub> (2.44 Å).<sup>89</sup> In **10**, the imidazole rings are essentially coplanar with the central As–As bond. Like **8**, the trans-bent geometry around the As–As bond may also be ascribed to the steric repulsion of the bulky NHC ligands because the **10-H** model is optimized in

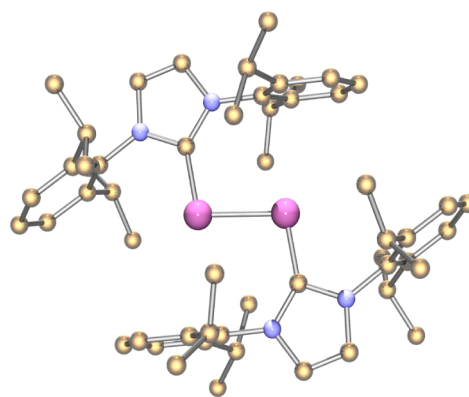


Figure 9. Molecular structure of **10**.

a gauche conformation with C<sub>2</sub> symmetry. Compound **10**, isostructural to **8**, may be regarded as a carbene–diarsinidene complex.<sup>88</sup> The As–C<sub>NHC</sub> bond distance of **10** [1.881(2) Å] is similar to those [1.899(3)–1.902(7) Å] for carbene–arsinidene complexes,<sup>90</sup> which is between the 2.018(3) Å As–C single-bond distance in L:AsCl<sub>3</sub> [L: = :C{N(2,6-Pr<sup>i</sup><sub>2</sub>C<sub>6</sub>H<sub>3</sub>)CH}<sub>2</sub>] and the typical As=C double-bond distances in acyclic arsaalkenes (1.816–1.827 Å).<sup>90</sup> Thus, the As–C bond in **10** has a partial double-bond feature. The pπ back-donation from the lone-pair orbital (with pure p character) of the arsenic atom to the empty p orbital of the carbene carbon atom is modest, which is consistent with the 1.341 WBI value of the As–C<sub>NHC</sub> bond in **10**.<sup>88</sup>

While the parallel syntheses of NHC-stabilized Sb<sub>2</sub> and Bi<sub>2</sub> through reduction of the corresponding L:ECl<sub>3</sub> (E = Sb and Bi) complexes have not yet been achieved,<sup>3</sup> Bertrand et al. recently reported the synthesis of CAAC-stabilized Sb<sub>2</sub> (as purple crystals in 45% yield) via potassium graphite reduction of the corresponding CAAC:SbCl<sub>3</sub> adduct.<sup>91</sup> Notably, controlled potassium graphite reduction was demonstrated. Consequently, CAAC-complexed SbCl<sub>2</sub> and SbCl intermediates can also be isolated. Similar to carbene-stabilized P<sub>2</sub> (**8** and **9**) and As<sub>2</sub> (**10**), CAAC-stabilized Sb<sub>2</sub> contains a 2.8125(10) Å Sb–Sb single bond. The WBI sequence of the E–C (E = P, As, and Sb) bonds in **8**, **10**, and CAAC-stabilized Sb<sub>2</sub> [i.e., P–C (1.397) > As–C (1.341) > Sb–C (1.234)] suggests a decreased multiplicity of the E–C bonds from **8** to (CAAC)<sub>2</sub>Sb<sub>2</sub>. This thus supports the description of (CAAC)<sub>2</sub>Sb<sub>2</sub> as a carbene-stabilized diatomic antimony.

## ■ REACTIVITY OF NHC-STABILIZED DIATOMIC MOLECULES

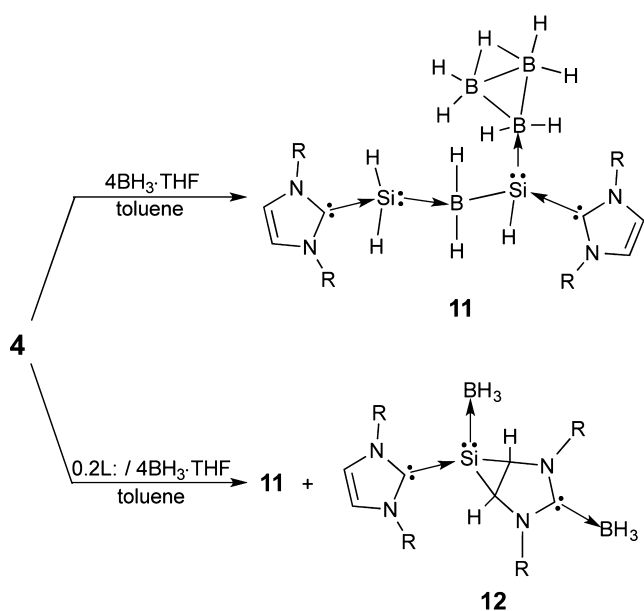
NHC-stabilized diatomics L:E–E:L [E = Si (**4**), P (**8** and **9**), and As (**10**)] were expected to demonstrate unusual reactivity because of their low-coordinate and electron-rich E<sub>2</sub> cores. Notably, the E<sub>2</sub> cores not only behave as Lewis acids (by accepting electron pairs from the carbenes), but also may function as Lewis bases (by donating electron pairs of the E<sub>2</sub> cores) to various Lewis acids.

Alkene/alkyne hydroboration is a classic organic reaction. However, the reactions of borane with the heavier silicon analogues of alkenes and alkynes have not been thoroughly investigated. The hydroboration reactions of disilenes (R<sub>2</sub>Si=SiR<sub>2</sub>) have only been theoretically explored.<sup>92</sup> Sekiguchi et al. group realized hydroboration of disilynes (RSi≡SiR, R = SiPr<sup>i</sup>[CH(SiMe<sub>3</sub>)<sub>2</sub>]<sub>2</sub>), giving boryl-substituted disilenes as the trans isomers.<sup>93,94</sup> In comparison with the low-oxidation-state

neutral silicon compounds such as silylenes, disilynes and disilynes, carbene-stabilized  $\text{Si}_2$  (**4**) is unique because it contains two types of reactive sites: the Si–Si double bond and the lone pair of electrons residing at each silicon atom. Thus, we were intrigued by the unexplored reactivity between **4** and  $\text{BH}_3$ .

Reaction of (pure crystalline) **4** with  $\text{BH}_3\cdot\text{THF}$  in a 1:4 molar ratio in toluene gives **11** in 72% yield (Scheme 5).<sup>71</sup> The

**Scheme 5.** Reaction of **4** with  $\text{BH}_3\cdot\text{THF}$  ( $\text{R} = 2,6$ -Diisopropylphenyl)



1:2 stoichiometric ratio of the reactants ( $4\text{-BH}_3\cdot\text{THF}$ ) would give the same major product **11** in a lower yield. Notably, the corresponding  $\text{BH}_3\cdot\text{THF}$  reaction of the mixture consisting of **4** and the free NHC ligand  $\text{L}$ : ( $4$  to  $\text{L}$ : = 5:1) leads to both **11** (30% yield) and **12** (28% yield) (Scheme 5), which can be readily separated because of their different solubilities in toluene.  $\text{SiH}_2$  is highly reactive and has been observed as an intermediate in the chemical vapor deposition of the silicon film via  $\text{SiH}_4$  pyrolysis.<sup>95</sup> Compound **11** represents the first “push–pull”-stabilized parent silylene ( $\text{SiH}_2$ ) that accepts electron donation from the carbene while donating an electron pair to the  $\text{L}:\text{Si}(\text{H})(\text{B}_3\text{H}_7)\text{BH}_2$  fragment.<sup>96</sup>

Rivard et al. subsequently synthesized  $\text{L}:\text{SiH}_2(\text{BH}_3)$  via  $\text{LiAlH}_4$  reduction of  $\text{L}:\text{SiCl}_2$  [ $\text{L} = :\text{C}\{\text{N}(2,6\text{-Pr}^i_2\text{C}_6\text{H}_3)\text{CH}_2\}_2$ ], which was then combined with  $\text{W}(\text{CO})_5\cdot\text{THF}$  to afford  $\text{L}:\text{SiH}_2[\text{W}(\text{CO})_5]$ .<sup>97</sup> Notably, the “push–pull”-stabilized heavier analogues of  $\text{SiH}_2$  (i.e.,  $\text{GeH}_2$  and  $\text{SnH}_2$ ) have also been achieved by Rivard et al.<sup>98–101</sup>

The X-ray structure of **11** (Figure 10) shows that the top reaction in Scheme 5, involving one equiv of **4** and four equiv of  $\text{BH}_3\cdot\text{THF}$ , results in cleavage of the  $\text{Si}=\text{Si}$  double bond in **4** with insertion of a  $\text{BH}_2$  unit between two silicon(II) atoms.<sup>71</sup> The  $\text{BH}_2$  fragment was not observed in the  $^1\text{H}$  NMR spectrum<sup>102</sup> but features a triplet at  $-50.4$  ppm in the proton-coupled  $^{11}\text{B}$  NMR spectrum. While three hydrogen atoms are transferred from boron to silicon atoms, the left  $\text{BH}_2$  fragments assemble into a neutral three-membered  $\text{B}_3\text{H}_7$  ring, which, as a Lewis acid, is bound to a borylsilylene center in **11**. The  $\text{B}_3\text{H}_7$  ring is also characterized by  $-0.29$  ppm broad  $^1\text{H}$  NMR singlet and  $-30.0$  ppm  $^{11}\text{B}$  NMR multiplet resonances.

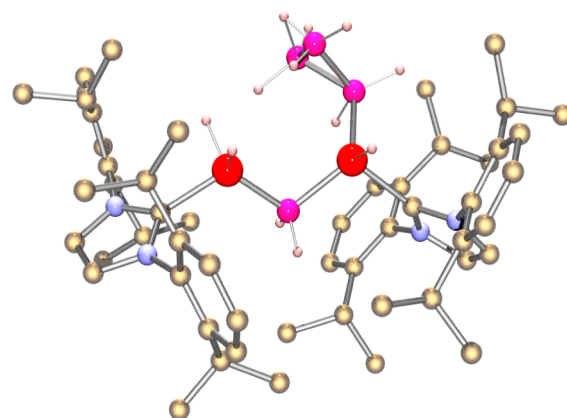


**Figure 10.** Molecular structure of **11**.

The  $^1\text{H}$  NMR chemical shift of the  $\text{B}_3\text{H}_7$  unit may be used to probe the electron-donating ability of different Lewis base ligands. For  $\text{L}:\text{B}_3\text{H}_7$  [ $\text{L} = \text{NH}_3$ , phosphines (i.e.,  $\text{PH}_3$ ,  $\text{MePH}_2$ ,  $\text{Me}_2\text{PH}$ ,  $\text{Me}_3\text{P}$ ), and **11**] complexes, the corresponding  $^1\text{H}$  NMR resonance of  $\text{B}_3\text{H}_7$  shifts to high field from 1.62 ppm ( $\text{L} = \text{NH}_3$ )<sup>103</sup> to 1.23–0.72 ppm ( $\text{L} =$  phosphines)<sup>104</sup> and then to  $-0.29$  ppm of **11**, indicating the increased electron-donating ability of the corresponding ligands.

All of the heteroatoms in the “zig-zag” C–Si–B–Si–C backbone of **11** have a distorted tetrahedral geometry.<sup>71</sup> The Si–C bond in **11** [1.934(4) and 1.944(4) Å] compares well to that in **4** [1.9271(15) Å]. While the central B(1) atom is disordered, the Si(1)–B(2) bond distance [1.965(7) Å] compares to the average Si(1)–B(1) (1.980 Å) and Si(2)–B(1) (1.902 Å) bond lengths. The WBI values of the Si(1)–B(1) (0.953), Si(2)–B(1) (0.999), and Si(1)–B(2) (0.869) bonds are supportive of typical single bonds. The natural charge distributions (from NBO analysis) [+0.95 for Si(1), +0.90 for Si(2),  $-0.92$  for B(1), and  $-1.03$  for  $\text{B}_3\text{H}_7$ ] suggest the donor–acceptor bond essences of the Si(2)–B(1) and Si(1)–B(2) bonds. The  $\text{SiH}$  and  $\text{SiH}_2$  units in **11** are characterized as a doublet (2.90 ppm) and a triplet (3.13 ppm) in the  $^1\text{H}$  NMR spectrum, respectively. The lack of  $^{29}\text{Si}$  resonances for **11** may be ascribed to the rapid quadrupolar relaxations of the neighboring boron atoms, which cause severe line broadening of the  $^{29}\text{Si}$  NMR signals.<sup>105</sup>

The formation of **12** clearly suggests that the presence of the free  $\text{L}$ : may affect the reaction pathway.<sup>71</sup> Although five- and six-membered cyclosilylenes have been well documented,<sup>106,107</sup> compound **12** represents the first “push–pull”-stabilized three-membered cyclosilylene (Figure 11). The formation of **12** may involve cycloaddition of the silicon(0) atom of an  $\text{L}:\text{Si}(\text{BH}_3)$  intermediate to the C=C backbone of an imidazole ring. Reactions of silicon(0) atoms with  $\pi$ -conjugate molecular systems indeed have been observed in matrix-isolation experiments.<sup>108,109</sup> With the addition of the silicon atom, the C=C double bond of the carbene is elongated to a C–C single bond [1.530(4) Å].<sup>71</sup> The dative Si(1)–C(28) bond [1.938(3) Å] is a little bit longer than those in the silylene ring [1.903(3) and 1.888(3) Å]. Like **11**, the  $^{29}\text{Si}$  NMR resonance of **12** cannot be observed. In the  $^1\text{H}$ -coupled  $^{11}\text{B}$  NMR spectrum of **12**, the  $-35.0$  ppm quartet resonance and  $-47.0$  ppm broad doublet resonance correspond to the  $\text{BH}_3$  units at the C(1) and Si(1) atoms, respectively.

In contrast to the hydroboration reactions of disilynes and disilynes,<sup>92–94</sup>  $\text{BH}_3$  is surprisingly able to cleave the  $\text{Si}=\text{Si}$

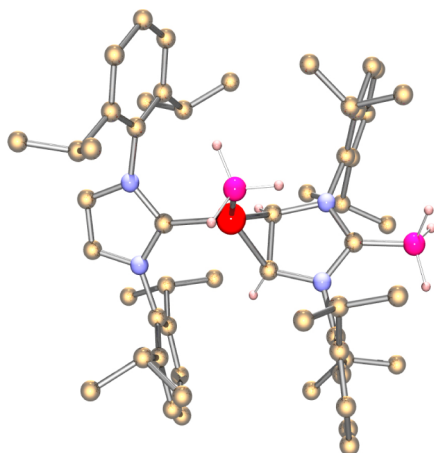


Figure 11. Molecular structure of 12.

double bond in 4, giving unexpected “push–pull”-stabilized silylene derivatives.

Compound 4 (i.e., IV in Figure 12) joins a small group of low-oxidation-state organosilicon compounds, I–III (Figure

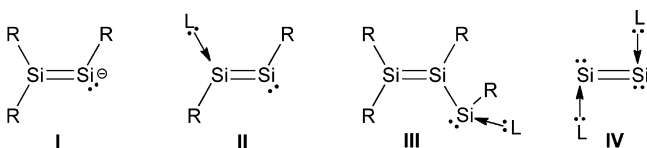
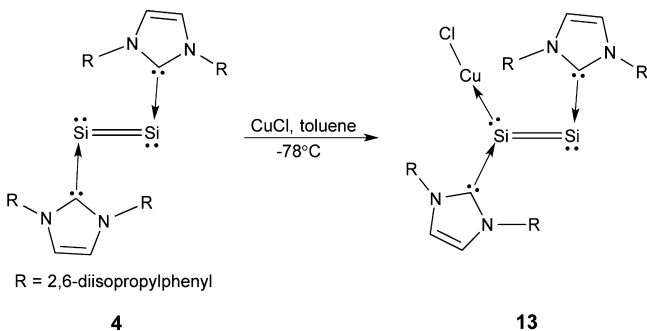


Figure 12.  $\sigma$ -donor compounds containing the Si=Si double bonds (L: = NHC): disilenides (I); NHC–disilyne complex (II); NHC-coordinated disilyl silylene (III); NHC-stabilized disilicon (IV).

12), which possess both Si–Si double bonds and silicon-based electron pairs.<sup>110–114</sup> On the basis of the  $\pi$ -donating capability of the Si=Si double bond and the  $\sigma$ -donor character of the silicon-based electron pair(s), compounds I–IV may serve as ligands to exhibit versatile coordination modes toward various metal salts. Considering the important roles of NHC–copper(I) complexes in catalysis and C–H bond activation,<sup>115,116</sup> we investigated the coordination behavior of 4 toward copper(I) chloride.<sup>72</sup>

Compound 13 was isolated as dark-purple-red crystals in 51% yield from the reaction of 4 with CuCl in toluene at  $-78^\circ\text{C}$  (Scheme 6). Compound 13 is thermally stable, surviving in boiling  $\text{C}_6\text{D}_6$ , but highly water-sensitive. In the presence of trace amounts of moisture, 13 decomposes to form L:CuCl [L: =  $:\text{C}\{\text{N}(2,6\text{-Pr}_2\text{C}_6\text{H}_3)\text{CH}\}_2$ ] as the major byproduct.

#### Scheme 6. Synthesis of 13



A higher yield of 13 can be achieved by combining 4 with CuCl in a 1:2 molar ratio, although 13 is a 1:1 adduct (4:CuCl). The fact that the 1:2 adduct was not observed may be attributed to the steric repulsion of the two bulky NHCs. The  $^{29}\text{Si}$  NMR resonance shifts downfield marginally from 224.5 ppm for 4 to 226.7 ppm for 13.

Only one of the two silicon atoms binds to CuCl in the solid state of 13 (Figure 13). The Si–Cu bond in 13 [2.2081(9) Å]

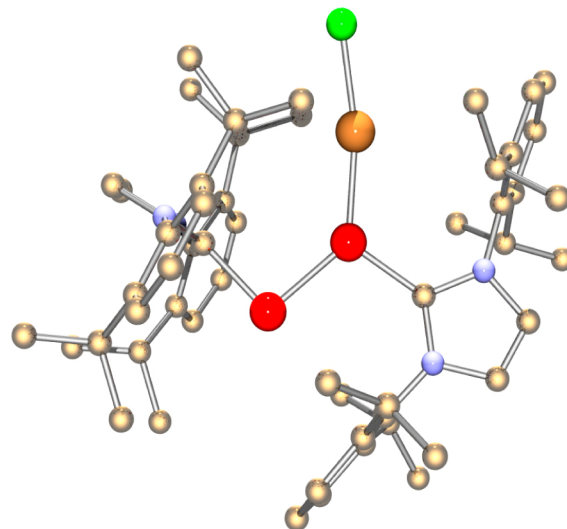


Figure 13. Molecular structure of 13.

compares well to those [2.2412(8) and 2.2458(8) Å] in lithium bis(disilyl)cuprate<sup>117</sup> and is less than the sum of the silicon and copper covalent radii (2.43 Å).<sup>118</sup> Coordination of CuCl to the  $\text{Si}_2$  core of 4 has an effect on the structure and bonding of the L:Si=Si:L unit.<sup>58,72</sup> The imidazole rings of the two NHCs in 4 are perpendicular to the  $\text{Si}_2$  core. However, in 13, only one imidazole ring retains this orientation. The other imidazole ring adjacent to the Si(1) atom is almost coplanar with the  $\text{Si}_2$  core [the N(2)–C(1)–Si(1)–Si(2) torsion angle =  $-0.72^\circ$ ], which favors  $\pi$ -electron delocalization of the  $\text{Si}_2$  core to the empty p orbital of the C(1) carbon atom. Indeed, in 13, the Si(1)–C(1) bond [1.917(3) Å] is slightly shorter than the Si(2)–C(28) bond [1.939(3) Å]. Moreover, in 13, the three-coordinate Si(1) atom adopts a trigonal-planar geometry, whereas the two-coordinate Si(2) atom, as those in 4 bearing lone pairs of electrons, has a bent geometry. The Si=Si double bond in 13 [2.2061(12) Å] is only about 0.02 Å shorter than that in 4 [2.2294(11) Å]. Its double-bond character is further endorsed by the 1.63 WBI of the Si–Si bond in model 13-Me [L: =  $:\text{C}\{\text{N}(\text{Me})\text{CH}\}_2$ ]. According to NBO analysis, in model 13-Me, the Si–Si  $\sigma$ -bonding orbital involves the overlap between the approximately  $\text{sp}^2$ -hybridized Si(1) atomic orbital (37.7% s, 62.0% p, and 0.3% d) and the Si(2) atomic orbital with predominant p character (17.4% s, 82.1% p, and 0.5% d). Meanwhile, the Si–Si  $\pi$  orbital has essentially pure p character (99.7%). While both the Si–Si  $\sigma$  and  $\pi$  bonds are somewhat polarized (about 55%) toward the Si(1) atom, the Si–Cu bond is more highly polarized (78%) toward silicon. The Si–Cu bond belongs to a single bond (WBI = 0.66).<sup>72</sup>

DFT computations on the 13-Me model also suggested that the carbene-stabilized  $\text{Si}_2$ –copper chloride complex may exist in two isomeric forms (see Figure 14). Notably, the  $\pi$  complex 13'-Me (optimized in  $\text{C}_2$  symmetry) is only 0.2 kcal/mol

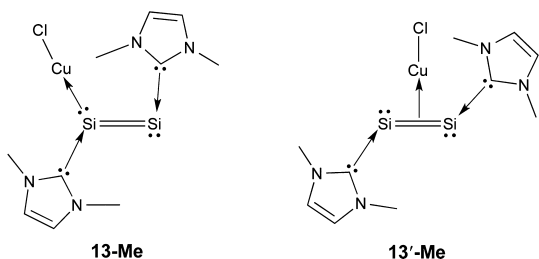


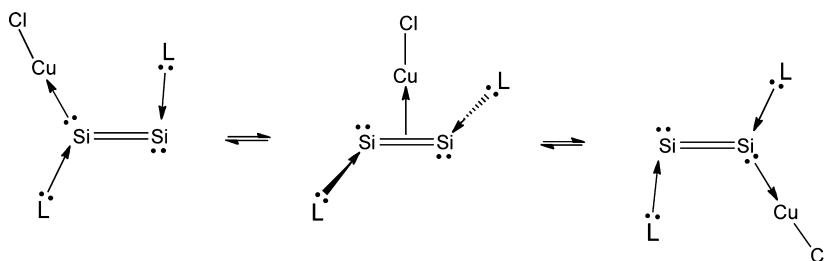
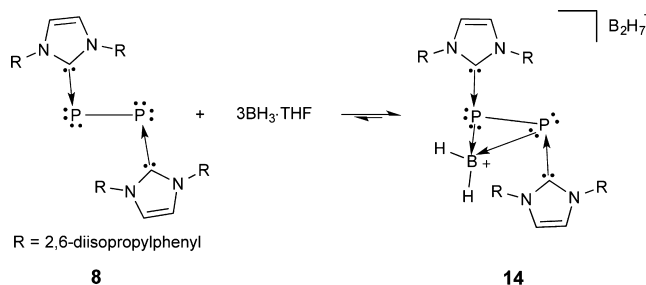
Figure 14. Isomers of 13.

higher in energy than the  $\sigma$ -complex minimum, **13-Me**. The side-on coordination of the  $L:Si=Si:L$  ligand ( $L = :C[N(Me)CH_2]$ ) to  $CuCl$  in **13'-Me** only results in about 0.06 Å elongation of the Si–Si distance with respect to that in **4**.<sup>58</sup> Indeed, the Si–Si bond distance in **13'-Me** (2.295 Å) is similar to those reported for disilene–transition metal  $\pi$  complexes.<sup>119</sup> It is worth noting that **13** only exhibited a singlet <sup>29</sup>Si NMR resonance. Moreover, the two carbene ligands are chemically equivalent in both <sup>1</sup>H and <sup>13</sup>C NMR spectra of **13**. All of these results suggest that in solution **13** may exist as the  $C_2$ -symmetric  $\pi$ -complex isomer or rapidly equilibrate at room temperature, very likely via a  $\pi$ -complex intermediate (Figure 15).

In order to study the dynamic complexation behavior of **13** in solution, variable-temperature (VT) <sup>1</sup>H NMR experiments were conducted. The sharp singlet resonance of the imidazole protons of **13** at 25 °C broadens and then splits into two separate peaks when cooled to –66 °C. Moreover, these VT spectral changes are reversible. These experimental observations may be due to either the slowing-down of the NHC ligand rotation around the  $C_{NHC}$ –Si axis in the symmetric  $\pi$ -complex form of **13** or the fact that the exchange (shown in Figure 15) is frozen out at low temperature.  $\sigma$ – $\pi$  rearrangements of organotransition-metal compounds are of great importance in catalytic processes.<sup>120</sup>

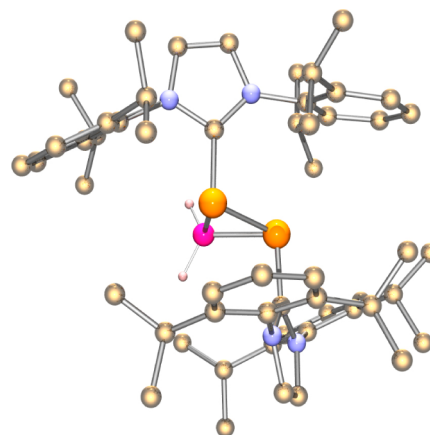
Because phosphorus has one more valence electron than silicon, carbene-stabilized  $P_2$  complexes (**8** and **9**),<sup>82</sup> containing a P–P singly bonded bis(phosphinidene) moiety, are expected to exhibit reactivities different from that of the carbene-stabilized  $Si_2$  (**4**).<sup>58</sup> While  $BH_3 \cdot THF$  is able to cleave the Si=Si double bond in **4**,<sup>71</sup> its reaction with **8** gives a dihydroboronium salt  $[L:P(\mu-BH_2)P:L]^+ \cdot B_2H_7^-$  (**14**), in which the L:P–P:L unit acts as a bidentate ligand to donate two electron pairs to the  $BH_2^+$  cation.<sup>121</sup>

Reaction of **8** with excess  $BH_3 \cdot THF$  gave (colorless) **14** in 85% yield. However, when the boronium complex **14** is dissolved in THF, it partially dissociates into **8** and  $BH_3 \cdot THF$  (Scheme 7) with a color change from colorless to orange red. The equilibrium lies to the right side of the reaction according

Figure 15. Proposed solution  $\sigma$ – $\pi$  interconversion of **13**.Scheme 7. Synthesis of **14**

to the molar ratio of **14** to **8** (4.5:1) in the equilibrium mixture. The presence of excess of  $BH_3 \cdot THF$  can effectively shift the equilibrium (Scheme 7) to the right side, significantly diminishing the dissociation of **14**.

Compound **14** features a  $P_2B$  three-membered ring (Figure 16).<sup>121</sup> The P–P bond distance in **14** [2.1993(11) Å] is almost

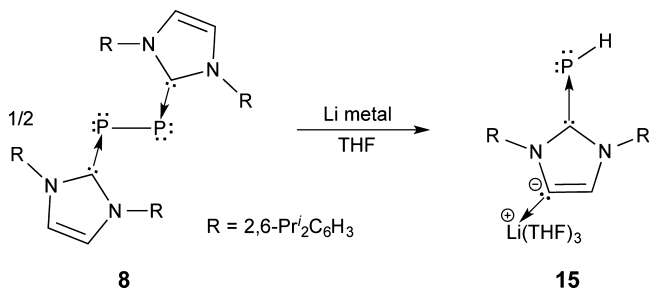
Figure 16. Molecular structure of **14**.

the same as that in **8** [2.2052(10) Å].<sup>82</sup> In addition, the C–P–P–C torsion angle in **14** (174.9°) is close to that in **8** (180°). However, the lone-pair orbital (with mainly p character) of the phosphorus atom in **14** involves the formation of the donor–acceptor P–B bond, instead of the  $p\pi$  back-donation to the empty p orbital of the carbene carbon atom as observed in **8**. Accordingly, the P–C bond of **14** [1.830(3) Å] is ca. 0.08 Å longer than that of **8** [1.7504(17) Å], which has somewhat multiple-bond character [WBI = 0.996 (**14**) vs 1.397 (**8**)]. The  $P_2$  unit in **14** is more electron-rich than that in **8** because the <sup>31</sup>P{<sup>1</sup>H} singlet resonance of **14** (–185.9 ppm) shifts upfield dramatically with respect to that for **8** (–53.3 ppm in THF-*d*<sub>6</sub>; –52.4 ppm in C<sub>6</sub>D<sub>6</sub>). The <sup>11</sup>B NMR resonance of the  $BH_2^+$  fragment in **14** (–31.6 ppm) is comparable to those for cyclic

bisphosphine boronium salts ( $-33$  to  $-37$  ppm).<sup>122</sup> The 0.930 WBI of the P–P bond in **14**, similar to that (1.004) of **8**, supports P–P single-bond essence. The P–B bonds of **14** [1.972(4) and 1.982(4) Å] are ca. 0.07 Å longer than those for a cyclic bisphosphine boronium salt ( $1.910 \pm 0.003$  Å).<sup>122</sup>

In addition to Lewis acids, we also explored the reactivity of L:P–P:L [**8**; L: = :C{N(2,6-Pr<sup>i</sup><sub>2</sub>C<sub>6</sub>H<sub>3</sub>)CH<sub>2</sub>}<sub>2</sub>] toward redox reagents. The lithium reduction of **8** results in the C<sub>4</sub>-lithiated NHC–parent phosphinidene complex L:PH (**15**; L: = :C{[N(2,6-Pr<sup>i</sup><sub>2</sub>C<sub>6</sub>H<sub>3</sub>)<sub>2</sub>CHLi(THF)<sub>3</sub>]} as yellow crystals in 16% yield (Scheme 8).<sup>87</sup> The formation of **15** involves lithium-mediated C–H bond activation of the imidazole ring and cleavage of the P–P core of **8**.

Scheme 8. Synthesis of **15**



Parent phosphinidene, PH, is highly reactive because of its triplet ground state with a 22 kcal/mol triplet/singlet energy gap.<sup>123</sup> Acyclic diaminocarbene–PH complexes were synthesized several decades ago.<sup>124–127</sup> Compound **15** represents the first experimentally realized NHC–PH adduct. While **15** contains an anionic NHC, the neutral NHC-based PH complex, L:PH [L: = :C{N(2,6-Pr<sup>i</sup><sub>2</sub>C<sub>6</sub>H<sub>3</sub>)CH<sub>2</sub>}<sub>2</sub>], was synthesized recently through NHC trapping of the PH species released from a fragile silylene–PH adduct.<sup>128</sup> Notably, the same carbene–PH complex may also be achieved via reaction of the corresponding imidazolium salt [L–H]<sup>+</sup>Cl<sup>–</sup> with the single phosphorus atom donors [i.e., Na(OCP) or P<sub>7</sub>(SiMe<sub>3</sub>)<sub>3</sub>].<sup>129</sup> Furthermore, it is worth noting that, besides carbene ligands, f-block metal centers may also be employed to stabilize PH.<sup>130</sup>

The presence of the PH fragment in **15** is confirmed by the 1.86 ppm [<sup>1</sup>J(PH) = 167 Hz] doublet resonance in the <sup>1</sup>H NMR spectrum and the  $-143.0$  ppm (<sup>1</sup>J = 171 Hz) doublet resonance in the <sup>1</sup>H-coupled <sup>31</sup>P NMR spectrum.<sup>87</sup> The four-coordinate lithium cation in **15** is solvated by three THF molecules (Figure 17). The natural charge distribution at lithium (+0.84) and PH (–0.21) supports the anionic character of the carbene fragment in **15**. However, the anionic character of the ligand in **15** does not render the obvious changes of the structural and electronic properties of **15** with respect to the neutral NHC–PH complexes.<sup>129</sup> The P–C bond distance [1.763(2) Å] in **15** compares well to those for the neutral NHC-stabilized PH complexes [NHC: = [CH(CH<sub>3</sub>)N]<sub>2</sub>C, 1.770 Å (computed);<sup>131</sup> NHC = :C{N(2,6-Pr<sup>i</sup><sub>2</sub>C<sub>6</sub>H<sub>3</sub>)CH<sub>2</sub>}<sub>2</sub>, 1.752(1) Å].<sup>129</sup> Like **8**, the P–C bond in **15** has modest double-bond character (WBI of model **15-H** = 1.332). However, the pronounced high-field <sup>31</sup>P resonance ( $-143.0$  ppm, <sup>1</sup>J = 171 Hz) of **15**, similar to that ( $-136.68$  ppm, <sup>1</sup>J = 164 Hz) of L:PH [L: = :C{N(2,6-Pr<sup>i</sup><sub>2</sub>C<sub>6</sub>H<sub>3</sub>)CH<sub>2</sub>}<sub>2</sub>],<sup>129</sup> supports the description of **15** as an anionic NHC-stabilized parent phosphinidene complex.

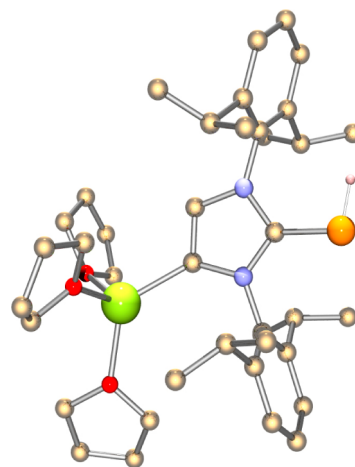
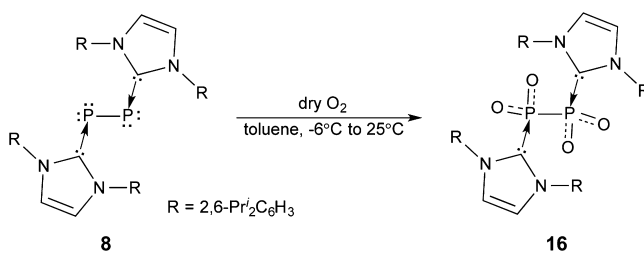


Figure 17. Molecular structure of **15**.

Recently, this group investigated the reactions of **8** with O<sub>2</sub>. It has been long documented that P<sub>4</sub>O<sub>n</sub> ( $n = 6, 7, 8, 9, 10$ ) oxides are stable and possess adamantane-like cage structures.<sup>42</sup> In contrast to isolable nitrogen oxides (i.e., NO, NO<sub>2</sub>, N<sub>2</sub>O, N<sub>2</sub>O<sub>3</sub>, N<sub>2</sub>O<sub>4</sub>, and N<sub>2</sub>O<sub>5</sub>), which are extensively related to our environment and many aspects of the human experience, the corresponding phosphorus congeners [i.e., PO, PO<sub>2</sub>, and P<sub>2</sub>O<sub>n</sub> ( $n = 1, 3, 4, 5$ )] are extremely reactive and typically studied in the gas phase or in matrix-isolation experiments.<sup>132</sup> Although transition metal–PO and –P<sub>2</sub>O complexes were reported several decades ago,<sup>133,134</sup> novel synthetic strategies are expected in order to develop the exciting chemistry of these highly reactive phosphorus oxides.

Inspired by the classic conversion of white phosphorus to P<sub>4</sub>O<sub>10</sub> oxide via combustion,<sup>42</sup> we allowed **8** to react with O<sub>2</sub> in toluene at temperatures from  $-6$  to  $+25$  °C, giving compound **16**, a carbene-stabilized P<sub>2</sub>O<sub>4</sub> complex, in 54% yield (Scheme 9).<sup>135</sup> While this reaction is extremely moisture- and temper-

Scheme 9. Synthesis of **16**



ature-sensitive, compound **16** is stable when exposed to air. Colorless X-ray-quality crystals of **16** and **16**·2H<sub>2</sub>O were obtained by recrystallization in toluene under a dry argon atmosphere or in air, respectively. Because single-electron oxidation has been observed for carbene-stabilized P<sub>2</sub> molecules (including **8**),<sup>136</sup> the splitting of triplet O<sub>2</sub> by the singlet P<sub>2</sub> core in **8** may involve a single-electron-transfer mechanism.<sup>137</sup>

Dinitrogen tetroxide, N<sub>2</sub>O<sub>4</sub>, exists in equilibrium with NO<sub>2</sub> at 25 °C (dissociation energy of N<sub>2</sub>O<sub>4</sub> = 14 kcal/mol).<sup>42</sup> However, carbene-complexed P<sub>2</sub>O<sub>4</sub> (**16**) is sufficiently stable such that dissociation to the carbene-stabilized PO<sub>2</sub> monomer was not observed (dissociation energy of **16** = 49 kcal/mol).<sup>135</sup> Like N<sub>2</sub>O<sub>4</sub> (a weakly N–N-bonded O<sub>2</sub>N–NO<sub>2</sub> dimer), the P<sub>2</sub>O<sub>4</sub> moiety in **16** exists as a P–P-bonded PO<sub>2</sub> dimer, which

adopts a trans-bent geometry because of carbene coordination (Figure 18). It is worth noting that  $P_2O_4$  itself energetically

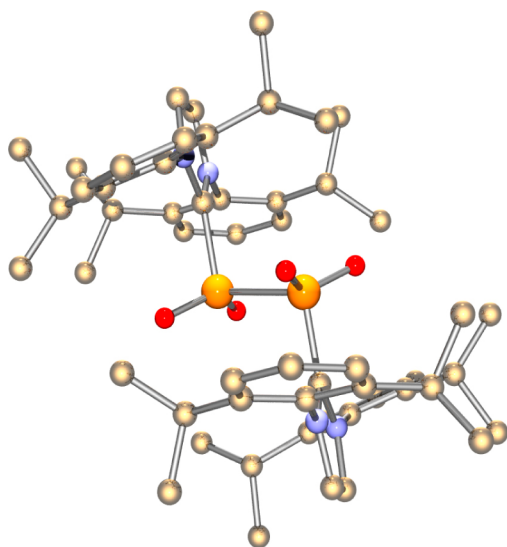


Figure 18. Molecular structure of 16.

favors an oxo-bridged and nonplanar  $O_2POPO$  structure (with  $C_s$  symmetry) rather than its  $O_2P-PO_2$  isomer.<sup>138,139</sup> The P–P bond of **16** [2.310(2) Å], the same as that [2.3103(7) Å] in a “Jack-in-the-Box” diphosphine,<sup>140</sup> is ca. 0.1 Å longer than that in **8** [2.2052(10) Å]. Meanwhile, the P–C single bond [1.895(3) Å] in **16** is about 0.13 Å longer than that [1.7504(17) Å] in **8**, which may attribute to the presence of P-to- $C_{NHC}$   $p\pi$  back-donation in **8**.<sup>82</sup> The P–O bond distances [1.466(3) and 1.470(3) Å] in **16** compare to the computed P–O bond distance (1.437 Å) in  $O_2P-PO_2$  ( $D_{2d}$  symmetry)<sup>138</sup> and the experimental P–O bond distances in  $L:P(O)_2Cl$  [1.452(2) Å,  $L = :C\{(Pr^i)NC(Me)\}_2$ ]<sup>141</sup> and in  $Ph_3PO$  (1.48 Å).<sup>142</sup> In contrast, it is obviously shorter than the P–OH bond distance [1.5750(15) Å] in  $L:P(O)_2OH$  [ $L = :C\{(Pr^i)NC(Me)\}_2$ ]<sup>143</sup> and the sum of phosphorus and oxygen covalent radii (1.73 Å).<sup>118</sup> The WBI values (1.14 Å, av) of the P–O bonds in the **16-H** model suggest modest multiple bond character of the P–O bonds. Regarding the  $PO_2$  fragment in the **16-H** model, the phosphorus atom bears +1.8 positive charge, while each oxygen holds about –1.10 negative charge. This suggests that in **16** the electron density is pulled away from the central phosphorus atoms by the more electronegative oxygen atoms. Consequently, the  $^1H$ -coupled  $^{31}P$  NMR singlet resonance of **16** shifts downfield obviously to 5.8 ppm with respect to that (–52.4 ppm) of **8**.

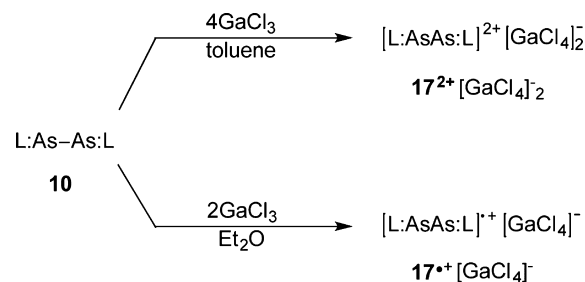
In a single crystal of  $16 \cdot 2H_2O$ , molecule **16** exhibits some changes of the structural parameters [ $d_{p-p} = 2.2132(13)$  Å;  $d_{p-o} = 1.458(2)$  and  $1.467(2)$  Å], which may be due to packing effects and the hydrogen-bonding interactions between lattice water molecules and **16**. The IR spectrum of **16** exhibits two characteristic  $PO_2$  stretching frequencies at  $1279\text{ cm}^{-1}$  (antisymmetric mode) and  $1061\text{ cm}^{-1}$  (symmetric mode), which compare well to the computed frequencies ( $1290$  and  $1061\text{ cm}^{-1}$ ) of  $PO_2$  for **16** ( $C_i$  symmetry), respectively. Notably, the stretching frequencies of  $PO_2$  for  $16 \cdot 2H_2O$  are red-shifted to  $1269\text{ cm}^{-1}$  (antisymmetric mode) and  $1057\text{ cm}^{-1}$  (symmetric mode), which may be due to the intermolecular hydrogen bonding between the lattice water and the oxygen atoms of the  $O_2P-PO_2$  core of **16**.<sup>135</sup> The direct oxidation of **8**

to **16** via  $O_2$  splitting suggests that our *carbene stabilization* strategy may be utilized for isolating compounds containing other highly reactive main-group oxide cores.

The main-group p-block elements are not inclined to undergo one-electron redox reactions.<sup>144</sup> Regarding the heavier group 15 elements, persistent<sup>145</sup> and stable<sup>145</sup> radicals have been mainly achieved for phosphorus.<sup>136,146–150</sup> The recent syntheses of the carbene-stabilized monocationic  $P_2^{\bullet+}$  radical and  $P_2^{2+}$  dication by Bertrand et al. are particularly interesting.<sup>136</sup> In contrast, the radical chemistry of arsenic, antimony, and bismuth is largely unexplored. Specifically, persistent arsenic-centered radicals have only been studied by gas-phase electron diffraction<sup>151</sup> and electron paramagnetic resonance (EPR) spectroscopy,<sup>147,152</sup>

Although gallium halides are poor-oxidizing reagents,<sup>153</sup> one-electron oxidation of the CAAC-stabilized parent borylene using  $GaCl_3$  as the oxidant has been reported.<sup>154</sup> When **10** was allowed to react with  $GaCl_3$  (in a 1:4 molar ratio) in toluene, the orange dicationic diarsene complex  $17^{2+}$  was quantitatively prepared. However, reaction of **10** with  $GaCl_3$  (in a 1:2 molar ratio) in  $Et_2O$  gave the green monocationic diarsenic radical  $17^{\bullet+}$  in 29.1% yield (Scheme 10),<sup>155</sup> which represents the only reported structurally characterized arsenic radical.<sup>51</sup>

#### Scheme 10. Gallium Chloride Oxidation of 10



Other group 13 chlorides,  $AlCl_3$  and  $InCl_3$ , may also oxidize **10** to the corresponding diarsene dications  $[L:As=As:L]^{2+}[ECl_4]_2^-$  [ $E = Al$  and  $In$ ;  $L = :C\{N(2,6-Pr^i_2C_6H_3)-CH\}_2$ ]. Notably, the  $[ECl_4]^-$  ( $E = Ga, Al$ , and  $In$ ) counteranions are relevant to the stability of the dicationic  $[L:As=As:L]^{2+}$  fragment in polar solvents. In acetonitrile,  $17^{2+}[ECl_4]_2^-$  ( $E = Al$  and  $Ga$ ) complexes are stable, whereas  $17^{2+}[InCl_4]_2^-$  gradually decomposes, with the color changing from orange to green.<sup>155</sup>

X-ray structural analysis of dark-green  $17^{\bullet+}$  crystals (Figure 19) shows that the  $As_2$  core of  $17^{\bullet+}$  is disordered with an average As–As bond distance of 2.32 Å, which is between the As–As single-bond distance in **10** [2.442(1) Å] and the As=As double-bond distance [2.224(2) Å] in  $RA_s=AsR'$  [ $R = 2,4,6-Bu^t_3C_6H_2$ ;  $R' = CH(SiMe_3)_2$ ]. The computed As–As bond distance (2.388 Å) of the simplified model  $17H^{\bullet+}$  [ $L = :C(NHCH)_2$ ; in  $C_2$  symmetry] is about 0.06 Å longer than that in  $17^{\bullet+}$ .<sup>155</sup>

The LMOs of the simplified  $17H^{\bullet+}$  model (Figure 20) suggest that, besides one lone-electron-pair orbital on each arsenic atom (b), the  $17H^{\bullet+}$  radical also contains one As–As  $\sigma$  bond (a), one As–As  $\pi$  bond (c), and one As–As  $\pi^*$  singly occupied molecular orbital (SOMO), which is consistent with the WBI (1.218) of the As–As bond. The  $As_2$  core of  $17H^{\bullet+}$  holds +0.18 positive charge, which is close to that (+0.16) of the  $P_2$  unit in the carbene-stabilized  $P_2^{\bullet+}$  radical.<sup>136</sup> Similar to the phosphorus analogue of  $17^{\bullet+}$ , the spin density distribution

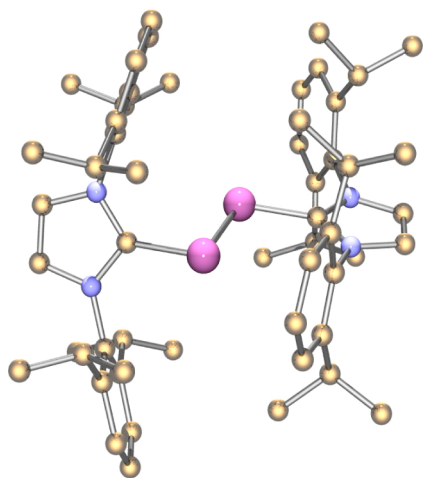


Figure 19. Molecular structure of  $17^{2+}$ .

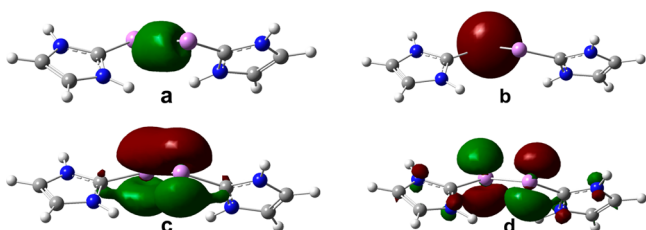


Figure 20. LMOs of  $17H^{2+}$  with  $C_2$  symmetry.

of  $17H^{2+}$  revealed that the unpaired electron was largely localized about the  $As_2$  core (0.41 at each arsenic atom). The room temperature EPR spectrum of  $17^{2+}$  in fluorobenzene displays a broadened septet ( $g \approx 2.05$ ), with poorly resolved low- and high-field hyperfine components, resulting from large hyperfine coupling with two equivalent  $^{75}As$  ( $I = 3/2$ ) nuclei ( $A \approx 68$  MHz). Using the correlation time estimated from parallel NMR studies ( $10^{-5}$  s), the spectrum is well simulated as a  $As_2$  radical involving equivalent arsenic atoms.

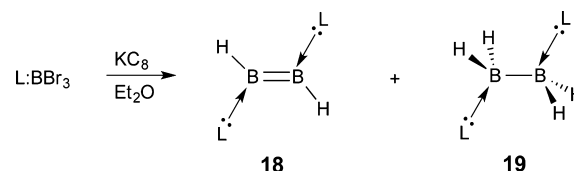
The As–As bond distance in  $17^{2+}$  [2.2803(5) Å] is about 0.16 Å shorter than that in **10** [2.442(1) Å] but only marginally shorter than that of  $17^{2+}$  (2.32 Å, av).<sup>155</sup> The 1.78 WBI for the As–As bond in the  $17H^{2+}$  model is supportive of the As=As double-bond character in  $17^{2+}$ . The +0.77 positive partial charge of the  $As_2$  core in  $17^{2+}$  compares well to that (+0.73) of the  $P_2$  unit in carbene-stabilized  $P_2^{2+}$ .<sup>136</sup>

### ■ NHC-STABILIZED DIBORENES, $Ga_6$ OCTAHEDRA, AND BERYLLIUM BOROHYDRIDE

Boron, the lightest group 13 element, is inclined to aggregate into various electron-deficient clusters and generally resists homonuclear multiple-bond formation.<sup>156</sup> The first breakthrough in the homonuclear multiple-bond chemistry of boron may be traced to the EPR observation of  $[R_2BBR_2]^{•-}$  radical anions in solution by Berndt and Klusik three decades ago.<sup>157</sup> Power et al. subsequently isolated the first structurally characterized stable radical anions  $[MeO(Mes)BB(Mes)OMe]^{•-}$  and  $[Mes_2BBMes(Ph)]^{•-}$  that contained a B–B one-electron  $\pi$  bond.<sup>158,159</sup> The same laboratory also experimentally realized the first dianionic compound containing a B=B double bond (i.e.,  $[Mes_2BB(Mes)Ph]^{2-}$ ),<sup>160</sup> consistent with the theoretical prediction of diborane dianions of Kaufmann and Schleyer.<sup>161</sup> Carbene-stabilized neutral dibor-

enes represent another type of stable compound containing boron–boron double bonds. In 2007, this laboratory synthesized the first NHC-stabilized neutral diborene (red),  $L:(H)B=B(H):L$  (**18**), and diborane (colorless),  $L:(H)_2B-B(H)_2:L$  (**19**) [ $L = :C\{N(2,6-Pr^i_2C_6H_3)CH\}_2$ ], by potassium graphite reduction of  $L:BBR_3$  (**20**) in diethyl ether (Scheme 11).<sup>162</sup>

Scheme 11. Synthesis of **18** and **19**



Hydrogen abstraction from ethereal solvents assisted by alkali metals may be involved in the formation of carbene-stabilized neutral diborene (**18**) and diborane (**19**). Otherwise, the formation of NHC-stabilized diboryne,  $L:B\equiv B:L$ , would have been expected.<sup>2</sup> Parent diborene  $HB=BH$ , with a triplet ground state and two one-electron  $\pi$  bonds, has been predicted to be highly reactive.<sup>163</sup> The successful isolation of **18** suggests that carbenes, as strong electron pair donors, may be extensively utilized in stabilizing a variety of elusive main-group molecules.

The X-ray structure of **18** shows that two NHCs coordinate to the  $HB=BH$  unit in a trans manner (Figure 21).<sup>162</sup> Like alkenes, the  $C_{NHC}(H)B=B(H)C_{NHC}$  core in diborene **18** is planar. The B=B double-bond distance in **18** (1.560 Å, av) compares to those of the diborane dianions (1.566–1.636 Å),<sup>160,164,165</sup> the computed values for  $HB=BH$  (1.498–1.515 Å),<sup>161</sup> and that for  $OC(H)B=B(H)CO$  (1.590 Å).<sup>166</sup> In contrast, the B–B bond in **19** (1.828 Å) belongs to a small group of relatively long single bonds, which is not only 0.27 Å longer than the B=B double bond in **18** (1.560 Å, av) but also longer than the B–B single bonds in three-coordinate diboron compounds (1.682–1.762 Å).<sup>167</sup>

The B–C bond distance of **18** (1.547 Å) is somewhat shorter than those for **19** (1.577 Å) and **20** (1.623 Å). The  $^{11}B$  NMR resonance of **18** shifts downfield to +25.3 ppm with respect to that (–31.6 ppm) of **19**.

Computations on the simplified model **18H** [ $L:(H)B=B(H):L$ ;  $L = :C(NHCH)_2$ ] supported the presence of a B=B double bond in **18**.<sup>162</sup> While the HOMO–1 possesses mixed B–B and B–H  $\sigma$ -bonding character, the HOMO largely involves B–B  $\pi$ -bonding interaction. The NBO study shows that the B–B  $\sigma$ - and  $\pi$ -bonding orbitals of **18H** have electron occupancies of 1.943 and 1.382, respectively. The 1.408 WBI of **18H**, although lower than 2.0, still document the B=B double-bond character in **18H**. The relatively low WBI value and electron occupancy of the B–B  $\pi$ -bonding orbital could be attributed to delocalization of the  $\pi$  electrons of boron atoms to the vacant p orbital of the carbene carbon atom.

When the less bulky NHC [i.e.,  $L' = :C\{N(2,4,6-Me_3C_6H_2)CH\}_2$ ] is employed,  $L':(H)B=B(H):L'$  (**21**) and  $L':(H)_2B-B(H)_2:L'$  (**22**) complexes are isolated.<sup>168</sup> Notably, in the solid state, **21** may exist as three polymorphs with a planar (**21a**), twisted (**21b**), or trans-bent (**21c**)  $C_{NHC}(H)B=B(H)C_{NHC}$  core, respectively (Figure 22).

While **21a** is more energetically favored than the other two in terms of DFT computations, the isolation of three polymorphs

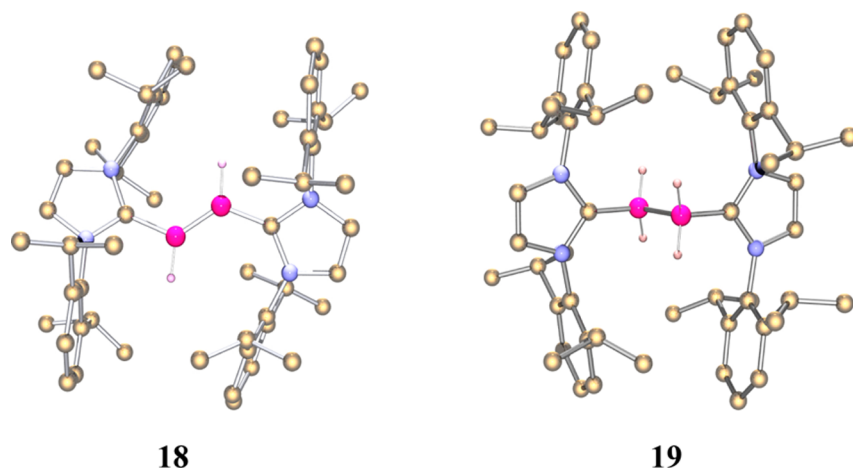


Figure 21. Molecular structure of 18 and 19.

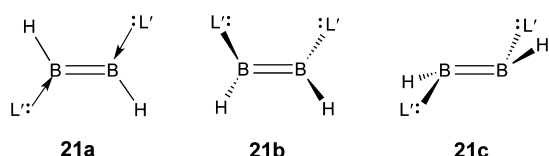


Figure 22. Conformational polymorphs of carbene-stabilized diborene 21.

of **21** may generally attribute to the flat potential energy surface for the  $C_{NHC}(H)B=B(H)C_{NHC}$  core of **21** and crystal-packing effects. The B=B bond distance in **21c** [1.679(9) Å] is longer than those in **21a** [1.602(5) Å] and **21b** [1.582(4) Å]. However, all of them are obviously shorter than the corresponding B–B single bond in **22** [1.795(5) Å]. The B=B double-bond character of **21** is also supported by the observed  $\pi_{B=B}-\pi^*_{B=B}$  absorption ( $\lambda = 574$  nm).<sup>168</sup>

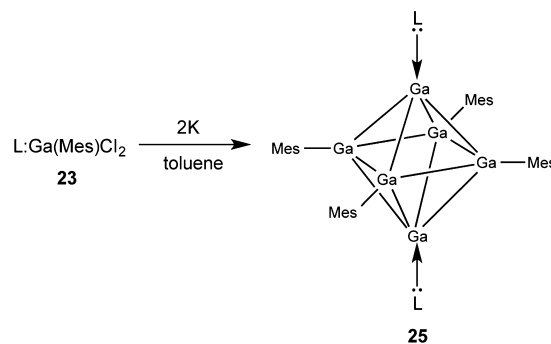
In addition to the parent diborene  $HB=BH$ , substituted diborenes may also be stabilized by carbenes. Braunschweig et al. recently isolated less bulky carbene-stabilized aryl-substituted diborenes, which may either coordinate to  $AgCl$  in the  $\eta^2$  mode<sup>169</sup> or undergo hydroboration reactions.<sup>170</sup> Indeed, the NHC-stabilized parent diborenes (**18** and **21**) may be regarded as the dimers of carbene–parent borylene ( $:BH$ ) complexes. While carbene-stabilized  $:BH$  is still a mystery,  $(CAAC)_2BH$  has been synthesized by Bertrand et al. via  $KC_8$  reduction of the corresponding  $CAAC:BBR_3$  precursor.<sup>154,171</sup> The strong  $\pi$ -acceptor ability of CAAC plays a key role in stabilizing elusive  $:BH$  species, which favors delocalization of the lone pair of electrons of the  $:BH$  moiety to the empty p orbital of the carbene carbon atom. CAAC-stabilized  $:BH$  only exhibits its basicity through one-electron oxidation and protonation of the central boron atom,<sup>154</sup> Interestingly, the very recently reported oxazol-2-ylidene-stabilized phenylborylene demonstrates the nucleophilicity by reaction with  $CF_3SO_3H$  and  $[(THF)Cr(CO)_5]$  to form the corresponding conjugate acid and a  $(CO)_5Cr$ -borylene complex, respectively.<sup>172</sup> This laboratory has attempted to target NHC-stabilized aminoborylene by potassium graphite reduction of carbene borenium complex  $[L:B(Cl)NPr_2]^+Cl^-$  [ $L: = :C\{N(2,6-Pr^i_2C_6H_3)CH\}_2$ ], which, however, is so reactive that the reduced boron center inserts into a benzylic C–H bond of the carbene (NHCs).<sup>3</sup>

The major barrier in the synthesis of carbene-stabilized  $B_2$  is hydrogen abstraction from the solvent media.<sup>162</sup> However, Braunschweig et al. overcame this obstacle by the sodium

naphthalenide reduction of  $L:(Br)_2B-B(Br)_2:L$  [ $L: = :C\{N(2,6-Pr^i_2C_6H_3)CH\}_2$ ] in THF, which was prepared by reaction of the carbene ( $L:$ ) with tetrabromodiborene(4).<sup>173</sup> The resulting major product,  $L:B\equiv B:L$ , unambiguously contains a  $B\equiv B$  triple bond [1.449(3) Å], which is about 0.11 Å longer than that for carbene-stabilized diborene **18** (1.560 Å, av).<sup>162</sup> The linear C–B–B–C core is also consistent with the theoretical results.<sup>174,175</sup> Meanwhile, the  $^{11}B$  NMR resonance of NHC-stabilized  $B_2$  shifts downfield to 39 ppm with respect to that of **18** (25 ppm).<sup>162</sup> While the carbene-based boron multiple bond chemistry is burgeoning, the heavier group 13 analogues such as  $L:EE:L$  and  $L:(H)EE(H):L$  ( $L: =$  carbene;  $E = Al, Ga,$  and  $In$ ) has yet to be experimentally realized. Indeed,  $L:(H)_2Al-Al(H)_2:L$  [ $L: = :C\{N(2,6-Pr^i_2C_6H_3)CH\}_2$ ], the analogue of **19**, has been synthesized by Stasch et al.

Reduction of  $L:Ga(Mes)Cl_2$  [**23**;  $L: = :C\{(Pr^i)NC(Me)\}_2$ ] proved very interesting.<sup>177</sup> When **23** was combined with potassium graphite (in a molar ratio of 1:3) in hexane, a pale-yellow  $[L:Ga(Mes)Cl]_2$  dimer containing a Ga–Ga bond (**24**) was isolated. However, it is surprising that potassium reduction of **23** in toluene (in a molar ratio of 1:2) resulted in the unexpected ligand cleavages and ensuing formation of the red  $L:Ga[Ga_4Mes_4]Ga:L$  octahedron, **25**, in low yield (Scheme 12).

Scheme 12. Synthesis of **25**



Compound **25** contains an octahedral  $Ga_6$  core that is well shielded by four mesityl ligands at the equatorial positions and two carbene ligands ( $L:$ ) at the axial positions (Figure 23).<sup>177</sup> Both **25** and the  $[Ga_6\{Si(CMe_3)_3\}_4(CH_2C_6H_5)_2]^{2-}$  dianion<sup>178</sup> have 14 skeleton electrons and thus obey the Wade–Mingos rules. The  $D_2$  symmetry of **25** is characterized by the presence

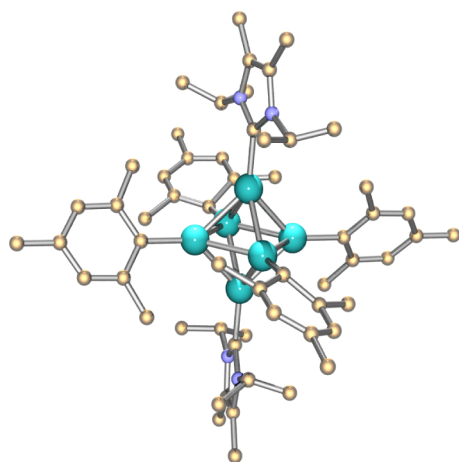


Figure 23. Molecular structure of 25.

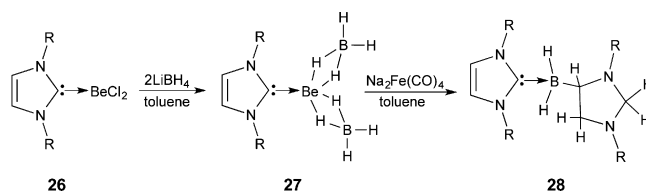
of three 2-fold axes through the Ga(1)⋯Ga(1A), Ga(2)⋯Ga(2A), and Ga(3)⋯Ga(3A) diagonals, respectively.<sup>177</sup> The Ga<sub>6</sub> core in **25** is aggregated by two axial gallium(0) atoms and four equatorial gallium(I) atoms. The axial Ga(3)⋯Ga(3a) distance (3.443 Å) is about 0.2 Å shorter than the equatorial Ga(1)⋯Ga(1a) (3.656 Å) and Ga(2)⋯Ga(2a) (3.671 Å) separations, indicating somewhat tetragonal compression of the Ga<sub>6</sub> octahedron core. The NICS<sup>6</sup> value (−10.2) for the simplified model L:Ga[Ga<sub>4</sub>Ph<sub>4</sub>]Ga:L (**25-H**; :L = :C{N(H)C(H)}<sub>2</sub>) suggests the aromatic character of **25**, which, though, is less than that (−27.3) for its parent octahedral dianion [Ga<sub>6</sub>H<sub>6</sub>]<sup>2−</sup>.<sup>177</sup>

Besides p-block elements, this laboratory is also engaged in exploring some of the challenging problems of group 2 alkaline-earth metals. It has been well documented that metal borohydrides are particularly attractive as potential alternative energy sources. Of these, beryllium borohydride, Be(BH<sub>4</sub>)<sub>2</sub>, has the highest hydrogen gas storage capacity,<sup>179</sup> but the precise manner in which it stores hydrogen remains unclear. Even the gas structure of the parent compound Be(BH<sub>4</sub>)<sub>2</sub> has been a puzzle for over 70 years.<sup>180</sup> Indeed, both bent and linear gas-phase structures for the B–Be–B fragment in Be(BH<sub>4</sub>)<sub>2</sub> have been suggested; however, neither the number nor disposition of the bridging hydrogen atoms have been established with certainty.<sup>181</sup> The helical polymeric structure of solid beryllium borohydride adds to the structural ambiguities.<sup>182,183</sup> Thus, we were compelled to find a facile means to stabilize and structurally characterize monomeric beryllium borohydride.

Beryllium borohydride is highly reactive and (even) explosive when exposed to air. Using carbene stabilization, we isolated the first structurally characterized monomeric Be(BH<sub>4</sub>)<sub>2</sub> complex [i.e., L:Be(BH<sub>4</sub>)<sub>2</sub> (**27**); L = :C{N(2,6-Pr<sup>i</sup><sub>2</sub>C<sub>6</sub>H<sub>3</sub>)CH<sub>2</sub>}<sub>2</sub>]. This compound survives in air for several days.<sup>184</sup>

NHC-stabilized beryllium chloride, L:BeCl<sub>2</sub> (**26**), was prepared in nearly quantitative yield by combining L: and BeCl<sub>2</sub> in hexane. Reaction of L:BeCl<sub>2</sub> with LiBH<sub>4</sub> affords carbene-stabilized beryllium borohydride **27** (Scheme 13; R = 2,6-Pr<sup>i</sup><sub>2</sub>C<sub>6</sub>H<sub>3</sub>) as colorless crystals in 67.8% yield. Compound **28** was prepared (in 64.3% yield) by allowing **27** to react with Na<sub>2</sub>[Fe(CO)<sub>4</sub>]·dioxane in toluene (Scheme 13). The formation of **28** involves both hydroboration of the C=C backbone of the imidazole ring and hydrogenation of the C(2) carbon of an NHC, which represents the first example of “dual reduction” of both the C=C backbone and the C(2) carbene center of an NHC ligand.<sup>185–188</sup>

### Scheme 13. Synthesis of 27 and 28



The beryllium atom in **27** is five-coordinate, adopting a distorted square-pyramidal geometry (Figure 24).<sup>184</sup> The

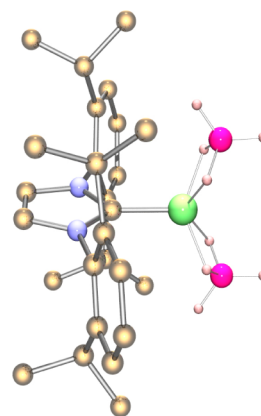


Figure 24. Molecular structure of 27.

1.765(2) Å Be–C bond distance in **27** is similar to that in **26** [1.773(5) Å]. With respect to the WBIs of the B–H bonds in the BH<sub>4</sub> units of **27** (0.87–0.99), the WBIs of the Be–C (0.22) and Be–H (0.07–0.08) bonds are pretty low, indicating the significant ionic character of these bonds in **27**. The natural charge distribution (−0.83 for each BH<sub>4</sub> unit and +1.53 for the beryllium atom) further confirms its dication character. Each [BH<sub>4</sub>]<sup>−</sup> anion binds to the Be<sup>2+</sup> center in a bidentate fashion through two bridging Be–H–B bonds. Both the Be⋯B distances (1.947 and 1.959 Å) and the B(1)–Be(1)–B(2) angle (121.7°) in **27** are similar to those of polymeric Be(BH<sub>4</sub>)<sub>2</sub> [1.918(4)–2.001(4) Å and 123.5–124.8°, respectively].<sup>183</sup> This nonlinear B–Be–B arrangement should attribute to carbene coordination. The average B–H bond distance (1.08 Å) in the [BH<sub>4</sub>]<sup>−</sup> units of **27** is comparable to that of polymeric Be(BH<sub>4</sub>)<sub>2</sub> (1.13 Å).<sup>183</sup> The proton-coupled <sup>11</sup>B NMR resonance of the [BH<sub>4</sub>]<sup>−</sup> units in **27** (a broad quintet at −31.2 ppm) is comparable to those for other metal borohydrides (LiBH<sub>4</sub>, −42.0 ppm),<sup>189</sup> corresponding to the 0.06 ppm singlet <sup>1</sup>H resonance in the <sup>1</sup>H{<sup>11</sup>B} NMR spectrum of **27**.

The X-ray structure (Figure 25) of **28** shows a BH<sub>2</sub> fragment bridged between C(1) of a nonreduced NHC and C(29) of a reduced carbene moiety. The ca. 1.615 Å B–C bond distances are marginally longer than those [1.588(7)–1.602(7) Å] in anionic N-heterocyclic dicarbene–BH<sub>3</sub> binuclear complexes.<sup>190</sup> As a result of hydroboration reaction, the C(29)–C(30) bond is elongated to 1.507(2) Å, corresponding to a typical C–C single bond.

Two <sup>1</sup>H resonances at 4.08 and 4.22 ppm of **28** are assigned to the two diastereotopic hydrogen atoms at the C(2) carbon [C(28)] of the imidazole ring, in accordance with the reported C(2) proton resonances (4.29 and 4.59 ppm) of similar saturated imidazolidines.<sup>185</sup> The proton-coupled <sup>11</sup>B NMR of

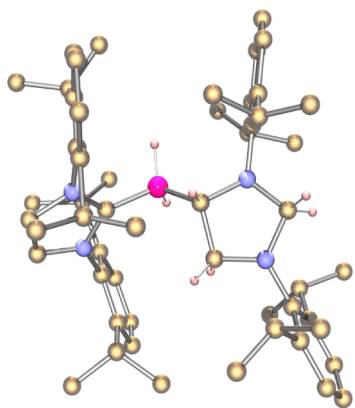


Figure 25. Molecular structure of 28.

28 (a broad singlet with shoulders at  $-25.5$  ppm) further supports the presence of the  $\text{BH}_2$  unit in 28.

Carbene-stabilized monomeric beryllium borohydride, 27, exhibits unusual reactivity toward  $\text{Na}_2[\text{Fe}(\text{CO})_4]\cdot\text{dioxane}$ , resulting in unique dual reduction of an imidazole ring. Further reactivity investigation of 27 is promising and may result in other amazing beryllium derivatives.

## CONCLUSIONS

Replacing *m*-terphenyl ligands with NHCs in our research program has significantly extended the kinetic stabilization strategy from unusual organogallium complexes (cyclogallenes and digallyne) to an extensive collection of novel main-group molecules. Recent studies clearly demonstrate that carbene-stabilized main-group diatomic allotropes are particularly intriguing not only because of their unusual structures and bonding, but also because of the unique platform they provide to access other amazing molecules. In addition, it is worth noting that the electronic and structural features of the stabilized main-group species are largely affected by the properties of the employed ligands. Thus, developing novel carbene ligand systems will facilitate new discoveries in this rapidly evolving field of N-heterocyclic carbene—main-group chemistry.

## AUTHOR INFORMATION

### Corresponding Author

\*E-mail: robinson@uga.edu.

### Notes

The authors declare no competing financial interest.

### Biographies



Gregory H. Robinson gained his B.S. (1980) in Chemistry from Jacksonville State University. In addition to studying Chemistry, he was also a standout on the Gamecock football team, earning All-American and Gulf South Conference Defensive Player of the Year honors. Robinson pursued graduate studies under the guidance of Professor Jerry L. Atwood at The University of Alabama. After obtaining his Ph.D. (1984), he joined the faculty of Clemson University and pursued a research program in main-group chemistry. Robinson joined the faculty of The University of Georgia in 1995, where he is now Foundation Distinguished Professor of Chemistry. He has served on numerous editorial boards including *Chemical & Engineering News*, *Organometallics*, and *Inorganic Chemistry*. Professor Robinson has received numerous honors including the Southern Chemist Award (1998), the Herty Medal (2008), the Humboldt Research Award (2012), and the F. Albert Cotton Award in Synthetic Inorganic Chemistry (2013), awarded by the American Chemical Society.



Yuzhong Wang received his B.S. (1993) and M.S. (1996) in Chemistry from Zhengzhou University and his Ph.D. (2003) from the University of Kentucky supervised by Professor David A. Atwood. After postdoctoral research in the laboratory of Professor Gregory H. Robinson at The University of Georgia, Wang now holds the title of Senior Research Scientist. His research interests concern the applications of carbenes in low-oxidation-state main-group chemistry.

## ACKNOWLEDGMENTS

We are grateful to the National Science Foundation for support from Grant CHE-1265212. We remain indebted to our talented co-workers and colleagues.

## REFERENCES

- (1) Quadbeck-Seeger, H.-J. *World of the Elements: Elements of the World*; Wiley: Weinheim, Germany, 2007.
- (2) Wang, Y.; Robinson, G. H. *Chem. Commun.* **2009**, 5201–5213.
- (3) Wang, Y.; Robinson, G. H. *Inorg. Chem.* **2011**, *50*, 12326–12337.
- (4) Wang, Y.; Robinson, G. H. *Dalton Trans.* **2012**, *41*, 337–345.
- (5) Robinson, G. H. *Acc. Chem. Res.* **1999**, *32*, 773–782.
- (6) Chen, Z.; Wannere Chaitanya, S.; Corminboeuf, C.; Puchta, R.; Schleyer, P. v. R. *Chem. Rev.* **2005**, *105*, 3842–3888.
- (7) Chen, Z.; Jiao, H.; Hirsch, A.; Schleyer, P. v. R. *Angew. Chem., Int. Ed.* **2002**, *41*, 4309–4312.
- (8) Chen, Z.; King, R. B. *Chem. Rev.* **2005**, *105*, 3613–3642.
- (9) Stock, A.; Pohland, E. *Ber. Dtsch. Chem. Ges. B* **1926**, *59B*, 2215–2223.
- (10) Breslow, R. *J. Am. Chem. Soc.* **1957**, *79*, 5318–5318.
- (11) Du, C.-J. F.; Hart, H.; Ng, K.-K. *J. Org. Chem.* **1986**, *51*, 3162–3165.
- (12) Ruhlandt-Senge, K.; Ellison, J. J.; Wehmschulte, R. J.; Pauer, F.; Power, P. P. *J. Am. Chem. Soc.* **1993**, *115*, 11353–11357.

- (13) Li, X.-W.; Pennington, W. T.; Robinson, G. H. *Organometallics* **1995**, *14*, 2109–2111.
- (14) Li, X.-W.; Pennington, W. T.; Robinson, G. H. *J. Am. Chem. Soc.* **1995**, *117*, 7578–7579.
- (15) Tsipis, C. A. *Coord. Chem. Rev.* **2005**, *249*, 2740–2762.
- (16) Xie, Y.; Schreiner, P. R.; Schaefer, H. F., III; Li, X.-W.; Robinson, G. H. *J. Am. Chem. Soc.* **1996**, *118*, 10635–10639.
- (17) Bursten, B. E.; Fenske, R. F. *Inorg. Chem.* **1979**, *18*, 1760–1765.
- (18) Twamley, B.; Power, P. P. *Angew. Chem., Int. Ed.* **2000**, *39*, 3500–3502.
- (19) Wiberg, N.; Blank, T.; Westerhausen, M.; Schneiderbauer, S.; Schnöckel, H.; Krossing, I.; Schnepf, A. *Eur. J. Inorg. Chem.* **2002**, 351–356.
- (20) Li, X.-W.; Xie, Y.; Schreiner, P. R.; Gripper, K. D.; Crittendon, R. C.; Campana, C. F.; Schaefer, H. F., III; Robinson, G. H. *Organometallics* **1996**, *15*, 3798–3803.
- (21) Wright, R. J.; Brynda, M.; Power, P. P. *Angew. Chem., Int. Ed.* **2006**, *45*, 5953–5956.
- (22) Su, J.; Li, X.-W.; Crittendon, R. C.; Robinson, G. H. *J. Am. Chem. Soc.* **1997**, *119*, 5471–5472.
- (23) Su, J.; Li, X.-W.; Robinson, G. H. *Chem. Commun.* **1998**, 2015–2016.
- (24) Pyykkö, P.; Riedel, S.; Patzschke, M. *Chem.—Eur. J.* **2005**, *11*, 3511–3520.
- (25) Xie, Y.; Grev, R. S.; Gu, J.; Schaefer, H. F.; Schleyer, P. v. R.; Su, J.; Li, X.-W.; Robinson, G. H. *J. Am. Chem. Soc.* **1998**, *120*, 3773–3780.
- (26) Xie, Y.; Schaefer, H. F.; Robinson, G. H. *Chem. Phys. Lett.* **2000**, *317*, 174–180.
- (27) Dagani, R. *Chem. Eng. News* **1997**, *75* (June 16), 9–10.
- (28) Dagani, R. *Chem. Eng. News* **1998**, *76* (March 16), 31–35.
- (29) Klinkhammer, K. W. *Angew. Chem., Int. Ed. Engl.* **1997**, *36*, 2320–2322.
- (30) Cotton, F. A.; Cowley, A. H.; Feng, X. *J. Am. Chem. Soc.* **1998**, *120*, 1795–1799.
- (31) Bytheway, I.; Lin, Z. *J. Am. Chem. Soc.* **1998**, *120*, 12133–12134.
- (32) Allen, T. L.; Fink, W. H.; Power, P. P. *J. Chem. Soc., Dalton Trans.* **2000**, 407–412.
- (33) Grützmacher, H.; Fässler, T. F. *Chem.—Eur. J.* **2000**, *6*, 2317–2325.
- (34) Grunenberg, J.; Goldberg, N. *J. Am. Chem. Soc.* **2000**, *122*, 6045–6047.
- (35) Takagi, N.; Schmidt, M. W.; Nagase, S. *Organometallics* **2001**, *20*, 1646–1651.
- (36) Ponec, R.; Yuzhakov, G.; Girones, X.; Frenking, G. *Organometallics* **2004**, *23*, 1790–1796.
- (37) Sekiguchi, A.; Kinjo, R.; Ichinohe, M. *Science* **2004**, *305*, 1755–1757.
- (38) Uhl, W. Z. *Naturforsch., B: Chem. Sci.* **1988**, *43*, 1113–1118.
- (39) Rivard, E.; Power, P. P. *Inorg. Chem.* **2007**, *46*, 10047–10064.
- (40) Li, X.-W.; Su, J.; Robinson, G. H. *Chem. Commun.* **1996**, 2683–2684.
- (41) Tolman, W. B., Ed. *Activation of Small Molecules: Organometallic and Bioinorganic Perspectives*; Wiley: New York, 2006; p 363.
- (42) Cotton, F. A.; Wilkinson, G.; Bochmann, M.; Murillo, C. *Advanced Inorganic Chemistry*, 6th ed.; Wiley: New York, 1998.
- (43) Huttner, G.; Sigwarth, B.; Scheidsteger, O.; Zsolnai, L.; Orama, O. *Organometallics* **1985**, *4*, 326–332.
- (44) *Gmelin Handbuch der anorganischen Chemie, Arsen*; Verlag Chemie: Weinheim, Germany, 1952; Vol. 17, p 476.
- (45) Van Zee, R. J.; Ferrante, R. F.; Weltner, W., Jr. *J. Chem. Phys.* **1985**, *83*, 6181–6187.
- (46) Carmalt, C. J.; Cowley, A. H. *Adv. Inorg. Chem.* **2000**, *50*, 1–32.
- (47) Carmalt, C. J. Main Group Carbenes. In *Encyclopedia of Inorganic Chemistry*, 2nd ed.; King, R. B., Ed.; Wiley & Sons: Chichester, U.K., 2005; p 6640.
- (48) Bourissou, D.; Guerret, O.; Gabbai, F. P.; Bertrand, G. *Chem. Rev.* **2000**, *100*, 39–91.
- (49) Martin, D.; Melaimi, M.; Soleilhavoup, M.; Bertrand, G. *Organometallics* **2011**, *30*, 5304–5313.
- (50) Martin, D.; Soleilhavoup, M.; Bertrand, G. *Chem. Sci.* **2011**, *2*, 389–399.
- (51) Martin, C. D.; Soleilhavoup, M.; Bertrand, G. *Chem. Sci.* **2013**, *4*, 3020–3030.
- (52) Yao, S.-L.; Xiong, Y.; Driess, M. *Organometallics* **2011**, *30*, 1748–1767.
- (53) Ghadwal, R. S.; Azhakar, R.; Roesky, H. W. *Acc. Chem. Res.* **2013**, *46*, 444–456.
- (54) Roesky, H. W. *J. Organomet. Chem.* **2013**, *730*, 57–62.
- (55) Wilson, D. J. D.; Dutton, J. L. *Chem.—Eur. J.* **2013**, *19*, 13626–13637.
- (56) Braunschweig, H.; Dewhurst, R. D. *Angew. Chem., Int. Ed.* **2013**, *52*, 3574–3583.
- (57) Prabusankar, G.; Sathyanarayana, A.; Suresh, P.; Naga Babu, C.; Srinivas, K.; Metla, B. P. R. *Coord. Chem. Rev.* **2014**, *269*, 96–133.
- (58) Wang, Y.; Xie, Y.; Wei, P.; King, R. B.; Schaefer, H. F., III; Schleyer, P. v. R.; Robinson, G. H. *Science* **2008**, *321*, 1069–1071.
- (59) Ghadwal, R. S.; Roesky, H. W.; Merkel, S.; Henn, J.; Stalke, D. *Angew. Chem., Int. Ed.* **2009**, *48*, 5683–5686.
- (60) Melaimi, M.; Soleilhavoup, M.; Bertrand, G. *Angew. Chem., Int. Ed.* **2010**, *49*, 8810–8849.
- (61) Mondal, K. C.; Samuel, P. P.; Roesky, H. W.; Aysin, R. R.; Leites, L. A.; Neudeck, S.; Luebben, J.; Dittrich, B.; Holzmann, N.; Hermann, M.; Frenking, G. *J. Am. Chem. Soc.* **2014**, *136*, 8919–8922.
- (62) Sidiropoulos, A.; Jones, C.; Stasch, A.; Klein, S.; Frenking, G. *Angew. Chem., Int. Ed.* **2009**, *48*, 9701–9704.
- (63) Jones, C.; Sidiropoulos, A.; Holzmann, N.; Frenking, G.; Stasch, A. *Chem. Commun.* **2012**, 48, 9855–9857.
- (64) Bonyhady, S. J.; Jones, C.; Nembenna, S.; Stasch, A.; Edwards, A. J.; McIntyre, G. J. *Chem.—Eur. J.* **2010**, *16*, 938–955.
- (65) Dutton, J. L.; Wilson, D. J. D. *Angew. Chem., Int. Ed.* **2012**, *51*, 1477–1480.
- (66) Li, Y.; Mondal, K. C.; Samuel, P. P.; Zhu, H.; Orben, C. M.; Panneerselvam, S.; Dittrich, B.; Schwederski, B.; Kaim, W.; Mondal, T.; Koley, D.; Roesky, H. W. *Angew. Chem., Int. Ed.* **2014**, *53*, 4168–4172.
- (67) Jin, L.; Melaimi, M.; Liu, L.; Bertrand, G. *Org. Chem. Front.* **2014**, *1*, 351–354.
- (68) Nimlos, M. R.; Harding, L. B.; Ellison, G. B. *J. Chem. Phys.* **1987**, *87*, 5116–5124.
- (69) Weidenbruch, M. In *The Chemistry of Organic Silicon Compounds*; Rappoport, Z., Apeloig, Y., Eds.; Wiley: Chichester, U.K., 2001; Vol. 3, pp 391–428.
- (70) Zhou, M.; Jiang, L.; Xu, Q. *J. Chem. Phys.* **2004**, *121*, 10474–10482.
- (71) Abraham, M. Y.; Wang, Y.; Xie, Y.; Wei, P.; Schaefer, H. F., III; Schleyer, P. v. R.; Robinson, G. H. *J. Am. Chem. Soc.* **2011**, *133*, 8874–8876.
- (72) Chen, M.; Wang, Y.; Xie, Y.; Wei, P.; Gilliard, R. J., Jr.; Schwartz, N. A.; Schaefer, H. F., III; Schleyer, P. v. R.; Robinson, G. H. *Chem.—Eur. J.* **2014**, *20*, 9208–9211.
- (73) Cowley, M. J.; Huch, V.; Scheschke, D. *Chem.—Eur. J.* **2014**, *20*, 9221–9224.
- (74) Dyker, C. A.; Bertrand, G. *Science* **2008**, *321*, 1050–1051.
- (75) Krapp, A.; Bickelhaupt, F. M.; Frenking, G. *Chem.—Eur. J.* **2006**, *12*, 9196–9216.
- (76) Lee, V. Y.; Sekiguchi, A., Eds. *Organometallic Compounds of Low-Coordinate Si, Ge, Sn, and Pb: From Phantom Species to Stable Compounds*; Wiley: Chichester, U.K., 2010; Chapter 5.
- (77) Caporali, M.; Gonsalvi, L.; Rossin, A.; Peruzzini, M. *Chem. Rev.* **2010**, *110*, 4178–4235.
- (78) Cossairt, B. M.; Piro, N. A.; Cummins, C. C. *Chem. Rev.* **2010**, *110*, 4164–4177.
- (79) Piro, N. A.; Figueroa, J. S.; McKellar, J. T.; Cummins, C. C. *Science* **2006**, *313*, 1276–1279.
- (80) Piro, N. A.; Cummins, C. C. *Inorg. Chem.* **2007**, *46*, 7387–7393.
- (81) Tofan, D.; Cummins, C. C. *Angew. Chem., Int. Ed.* **2010**, *49*, 7516–7518.

- (82) Wang, Y.; Xie, Y.; Wei, P.; King, R. B.; Schaefer, H. F., III; Schleyer, P. v. R.; Robinson, G. H. *J. Am. Chem. Soc.* **2008**, *130*, 14970–14971.
- (83) Masuda, J. D.; Schoeller, W. W.; Donnadiou, B.; Bertrand, G. *Angew. Chem., Int. Ed.* **2007**, *46*, 7052–7055.
- (84) Masuda, J. D.; Schoeller, W. W.; Donnadiou, B.; Bertrand, G. *J. Am. Chem. Soc.* **2007**, *129*, 14180–14181.
- (85) Back, O.; Kuchenbeiser, G.; Donnadiou, B.; Bertrand, G. *Angew. Chem., Int. Ed.* **2009**, *48*, 5530–5533.
- (86) Weber, L. *Eur. J. Inorg. Chem.* **2000**, 2425–2441.
- (87) Wang, Y.; Xie, Y.; Abraham, M. Y.; Gilliard, R. J., Jr.; Wei, P.; Schaefer, H. F., III; Schleyer, P. v. R.; Robinson, G. H. *Organometallics* **2010**, *29*, 4778–4780.
- (88) Abraham, M. Y.; Wang, Y.; Xie, Y.; Wei, P.; Schaefer, H. F., III; Schleyer, P. v. R.; Robinson, G. H. *Chem.—Eur. J.* **2010**, *16*, 432–435.
- (89) Maxwell, L. R.; Hendricks, S. B.; Mosley, V. M. *J. Chem. Phys.* **1935**, *3*, 699–709.
- (90) Arduengo, A. J., III; Calabrese, J. C.; Cowley, A. H.; Dias, H. V. R.; Goerlich, J. R.; Marshall, W. J.; Riegel, B. *Inorg. Chem.* **1997**, *36*, 2151–2158.
- (91) Kretschmer, R.; Ruiz, D. A.; Moore, C. E.; Rheingold, A. L.; Bertrand, G. *Angew. Chem., Int. Ed.* **2014**, *53*, 8176–8179.
- (92) Xu, Y.-J.; Zhang, Y.-F.; Li, J.-Q. *Chem. Phys. Lett.* **2006**, *421*, 36–41.
- (93) Takeuchi, K.; Ikoshi, M.; Ichinohe, M.; Sekiguchi, A. *J. Am. Chem. Soc.* **2010**, *132*, 930–931.
- (94) Takeuchi, K.; Ichinohe, M.; Sekiguchi, A. *Organometallics* **2011**, *30*, 2044–2050.
- (95) Koecher, T.; Kerst, C.; Friedrichs, G.; Temps, F. The gas-phase oxidation of silyl radicals by molecular oxygen: Kinetics and mechanisms. In *Silicon Chemistry*; Jutzi, P., Schubert, U., Eds.; Wiley-VCH: Weinheim, Germany, 2003; pp 44–57.
- (96) Inoue, S.; Driess, M. *Angew. Chem., Int. Ed.* **2011**, *50*, 5614–5615.
- (97) Al-Rafia, S. M. I.; Malcolm, A. C.; McDonald, R.; Ferguson, M. J.; Rivard, E. *Chem. Commun.* **2012**, *48*, 1308–1310.
- (98) Thimer, K. C.; Al-Rafia, S. M. I.; Ferguson, M. J.; McDonald, R.; Rivard, E. *Chem. Commun.* **2009**, 7119–7121.
- (99) Al-Rafia, S. M. I.; Malcolm, A. C.; Liew, S. K.; Ferguson, M. J.; Rivard, E. *J. Am. Chem. Soc.* **2011**, *133*, 777–779.
- (100) Rivard, E. *Dalton Trans.* **2014**, *43*, 8577–8586.
- (101) Swarnakar, A. K.; McDonald, S. M.; Deutsch, K. C.; Choi, P.; Ferguson, M. J.; McDonald, R.; Rivard, E. *Inorg. Chem.* **2014**, *53*, 8662–8671.
- (102) Kajiwara, T.; Takeda, N.; Sasamori, T.; Tokitoh, N. *Organometallics* **2004**, *23*, 4723–4734.
- (103) Yoon, C. W.; Carroll, P. J.; Sneddon, L. G. *J. Am. Chem. Soc.* **2009**, *131*, 855–864.
- (104) Bishop, V. L.; Kodama, G. *Inorg. Chem.* **1981**, *20*, 2724–2727.
- (105) Arp, H.; Marschner, C.; Baumgartner, J. *Dalton Trans.* **2010**, *39*, 9270–9274.
- (106) Hill, N. J.; West, R. *J. Organomet. Chem.* **2004**, *689*, 4165–4183.
- (107) Kira, M.; Ishida, S.; Iwamoto, T.; Kabuto, C. *J. Am. Chem. Soc.* **1999**, *121*, 9722–9723.
- (108) Maier, G.; Reisenauer, H. P.; Egenolf, H. *Eur. J. Org. Chem.* **1998**, 1313–1317.
- (109) Maier, G.; Reisenauer, H. P. *Eur. J. Org. Chem.* **2003**, 479–487.
- (110) Scheschkewitz, D. *Chem. Lett.* **2011**, *40*, 2–11.
- (111) Scheschkewitz, D. *Angew. Chem., Int. Ed.* **2004**, *43*, 2965–2967.
- (112) Cowley, M. J.; Huch, V.; Rzepa, H. S.; Scheschkewitz, D. *Nat. Chem.* **2013**, *5*, 876–879.
- (113) Ichinohe, M.; Sanuki, K.; Inoue, S.; Sekiguchi, A. *Organometallics* **2004**, *23*, 3088–3090.
- (114) Yamaguchi, T.; Sekiguchi, A.; Driess, M. *J. Am. Chem. Soc.* **2010**, *132*, 14061–14063.
- (115) Gaillard, S.; Cazin, C. S. J.; Nolan, S. P. *Acc. Chem. Res.* **2012**, *45*, 778–787.
- (116) Egbert, J. D.; Cazin, C. S. J.; Nolan, S. P. *Catal. Sci. Technol.* **2013**, *3*, 912–926.
- (117) Cowley, M. J.; Abersfelder, K.; White, A. J. P.; Majumdar, M.; Scheschkewitz, D. *Chem. Commun.* **2012**, *48*, 6595–6597.
- (118) Cordero, B.; Gomez, V.; Platero-Prats, A. E.; Reves, M.; Echeverria, J.; Cremades, E.; Barragan, F.; Alvarez, S. *Dalton Trans.* **2008**, 2832–2838.
- (119) Kira, M. *Proc. Jpn. Acad., Ser. B* **2012**, *88*, 167–191.
- (120) Tsutsui, M.; Courtney, A.  $\sigma$ - $\pi$  Rearrangements of organo-transition metal compounds. In *Advances in Organometallic Chemistry*; Stone, F. G. A., West, R., Eds.; Elsevier: New York, 1977; Vol. 16, pp 241–282.
- (121) Wang, Y.; Xie, Y.; Abraham, M. Y.; Wei, P.; Schaefer, H. F., III; Schleyer, P. v. R.; Robinson, G. H. *Chem. Commun.* **2011**, *47*, 9224–9226.
- (122) Owsianik, K.; Chauvin, R.; Balinska, A.; Wiczorek, M.; Cypriak, M.; Mikolajczyk, M. *Organometallics* **2009**, *28*, 4929–4937.
- (123) Zittel, P. F.; Lineberger, W. C. *J. Chem. Phys.* **1976**, *65*, 1236–1243.
- (124) Issleib, K.; Leissring, E.; Riemer, M.; Oehme, H. *Z. Chem.* **1983**, *23*, 99–100.
- (125) Chernega, A. N.; Antipin, M. Y.; Struchkov, Y. T.; Sarina, T. V.; Romanenko, V. D. *Zh. Strukt. Khim.* **1986**, *27*, 78–82.
- (126) Chernega, A. N.; Ruban, A. V.; Romanenko, V. D.; Markovskii, L. N.; Korkin, A. A.; Antipin, M. Y.; Struchkov, Y. T. *Heteroat. Chem.* **1991**, *2*, 229–241.
- (127) Le Floch, P. *Coord. Chem. Rev.* **2006**, *250*, 627–681.
- (128) Hansen, K.; Szilvasi, T.; Blom, B.; Inoue, S.; Epping, J.; Driess, M. *J. Am. Chem. Soc.* **2013**, *135*, 11795–11798.
- (129) Tondreau, A. M.; Benko, Z.; Harmer, J. R.; Gruetzmacher, H. *Chem. Sci.* **2014**, *5*, 1545–1554.
- (130) Gardner, B. M.; Balazs, G.; Scheer, M.; Tuna, F.; McInnes, E. J. L.; McMaster, J.; Lewis, W.; Blake, A. J.; Liddle, S. T. *Angew. Chem., Int. Ed.* **2014**, *53*, 4484–4488.
- (131) Frison, G.; Sevin, A. *J. Organomet. Chem.* **2002**, *643*–*644*, 105–111.
- (132) Mielke, Z.; McCluskey, M.; Andrews, L. *Chem. Phys. Lett.* **1990**, *165*, 146–154.
- (133) Scherer, O. J.; Braun, J.; Walther, P.; Heckmann, G.; Wolmershaeuser, G. *Angew. Chem., Int. Ed.* **1991**, *30*, 852–854.
- (134) Scherer, O. J.; Weigel, S.; Wolmershaeuser, G. *Angew. Chem., Int. Ed.* **1999**, *38*, 3688–3689.
- (135) Wang, Y.; Xie, Y.; Wei, P.; Schaefer, H. F., III; Schleyer, P. v. R.; Robinson, G. H. *J. Am. Chem. Soc.* **2013**, *135*, 19139–19142.
- (136) Back, O.; Donnadiou, B.; Parameswaran, P.; Frenking, G.; Bertrand, G. *Nat. Chem.* **2010**, *2*, 369–373.
- (137) Borovik, A. S.; Zinn, P. J.; Zart, M. K. Dioxxygen Binding and Activation: Reactive Intermediates. In *Activation of Small Molecules: Organometallic and Bioinorganic Perspectives*; Tolman, W. B., Ed.; Wiley-VCH: Weinheim, Germany, 2006; p 187.
- (138) Lohr, L. L., Jr. *J. Phys. Chem.* **1990**, *94*, 1807–1811.
- (139) Bauschlicher, C. W., Jr.; Zhou, M.; Andrews, L. *J. Phys. Chem. A* **2000**, *104*, 3566–3571.
- (140) Hinchley, S. L.; Morrison, C. A.; Rankin, D. W. H.; Macdonald, C. L. B.; Wiacek, R. J.; Cowley, A. H.; Lappert, M. F.; Gundersen, G.; Clyburne, J. A. C.; Power, P. P. *Chem. Commun.* **2000**, 2045–2046.
- (141) Kuhn, N.; Stroebel, M.; Walker, M. *Z. Anorg. Allg. Chem.* **2003**, *629*, 180–181.
- (142) Goggin, P. L. In *Comprehensive Coordination Chemistry*; Wilkinson, G., Gillard, R. D., McCleverty, J. A., Eds.; Pergamon: Oxford, U.K., 1987; Vol. 2.
- (143) Kuhn, N.; Eichele, K.; Walker, M.; Berends, T.; Minkwitz, R. *Z. Anorg. Allg. Chem.* **2002**, *628*, 2026–2032.
- (144) Power, P. P. *Chem. Rev.* **2003**, *103*, 789–809.
- (145) Hicks, R. G. *Stable Radicals: Fundamentals and Applied Aspects of Odd-Electron Compounds*; John Wiley & Sons: Chichester, U.K., 2010; Chapter 10.

- (146) Sasamori, T.; Mieda, E.; Nagahora, N.; Sato, K.; Shiomi, D.; Takui, T.; Hosoi, Y.; Furukawa, Y.; Takagi, N.; Nagase, S.; Tokitoh, N. *J. Am. Chem. Soc.* **2006**, *128*, 12582–12588.
- (147) Gynane, M. J. S.; Hudson, A.; Lappert, M. F.; Power, P. P.; Goldwhite, H. *J. Chem. Soc., Chem. Commun.* **1976**, 623–624.
- (148) Agarwal, P.; Piro, N. A.; Meyer, K.; Mueller, P.; Cummins, C. *C. Angew. Chem., Int. Ed.* **2007**, *46*, 3111–3114.
- (149) Ishida, S.; Hirakawa, F.; Iwamoto, T. *J. Am. Chem. Soc.* **2011**, *133*, 12968–12971.
- (150) Back, O.; Celik, M. A.; Frenking, G.; Melaimi, M.; Donnadieu, B.; Bertrand, G. *J. Am. Chem. Soc.* **2010**, *132*, 10262–10263.
- (151) Hinchley, S. L.; Morrison, C. A.; Rankin, D. W. H.; Macdonald, C. L. B.; Wiacek, R. J.; Voigt, A.; Cowley, A. H.; Lappert, M. F.; Gundersen, G.; Clyburne, J. A. C.; Power, P. P. *J. Am. Chem. Soc.* **2001**, *123*, 9045–9053.
- (152) Gynane, M. J. S.; Hudson, A.; Lappert, M. F.; Power, P. P.; Goldwhite, H. *J. Chem. Soc., Dalton Trans.* **1980**, 2428–2433.
- (153) Wulfsberg, G. *Principles of Descriptive Inorganic Chemistry*; Brooks/Cole: Monterey, CA, 1987; p 461 pp.
- (154) Kinjo, R.; Donnadieu, B.; Celik, M. A.; Frenking, G.; Bertrand, G. *Science* **2011**, *333*, 610–613.
- (155) Abraham, M. Y.; Wang, Y.; Xie, Y.; Gilliard, R. J.; Wei, P.; Vaccaro, B. J.; Johnson, M. K.; Schaefer, H. F., III; Schleyer, P. v. R.; Robinson, G. H. *J. Am. Chem. Soc.* **2013**, *135*, 2486–2488.
- (156) Driess, M., Noeth, H., Eds. *Molecular Clusters of the Main Group Elements*; Wiley-VCH: Weinheim, Germany, 2004; p 444.
- (157) Klusik, H.; Berndt, A. *Angew. Chem., Int. Ed. Engl.* **1981**, *20*, 870–871.
- (158) Grigsby, W. J.; Power, P. P. *Chem. Commun.* **1996**, 2235–2236.
- (159) Grigsby, W. J.; Power, P. *Chem.—Eur. J.* **1997**, *3*, 368–375.
- (160) Moezzi, A.; Olmstead, M. M.; Power, P. P. *J. Am. Chem. Soc.* **1992**, *114*, 2715–2717.
- (161) Kaufmann, E.; Schleyer, P. v. R. *Inorg. Chem.* **1988**, *27*, 3987–3992.
- (162) Wang, Y.; Quillian, B.; Wei, P.; Wannere, C. S.; Xie, Y.; King, R. B.; Schaefer, H. F., III; Schleyer, P. v. R.; Robinson, G. H. *J. Am. Chem. Soc.* **2007**, *129*, 12412–12413.
- (163) Dill, J. D.; Schleyer, P. v. R.; Pople, J. A. *J. Am. Chem. Soc.* **1975**, *97*, 3402–3409.
- (164) Moezzi, A.; Bartlett, R. A.; Power, P. P. *Angew. Chem., Int. Ed. Engl.* **1992**, *104*, 1082–1083.
- (165) Noth, H.; Knizek, J.; Ponikvar, W. *Eur. J. Inorg. Chem.* **1999**, 1931–1937.
- (166) Wang, Z.-X.; Chen, Z.; Jiao, H.; Schleyer, P. v. R. *J. Theor. Comput. Chem.* **2005**, *4*, 669–688.
- (167) Moezzi, A.; Olmstead, M. M.; Power, P. P. *J. Chem. Soc., Dalton Trans.* **1992**, 2429–2434.
- (168) Wang, Y.; Quillian, B.; Wei, P.; Xie, Y.; Wannere, C. S.; King, R. B.; Schaefer, H. F., III; Schleyer, P. v. R.; Robinson, G. H. *J. Am. Chem. Soc.* **2008**, *130*, 3298–3299.
- (169) Bissinger, P.; Braunschweig, H.; Damme, A.; Kupfer, T.; Vargas, A. *Angew. Chem., Int. Ed.* **2012**, *51*, 9931–9934.
- (170) Braunschweig, H.; Dewhurst, R. D.; Hoerl, C.; Phukan, A. K.; Pinzner, F.; Ullrich, S. *Angew. Chem., Int. Ed.* **2014**, *53*, 3241–3244.
- (171) Wang, Y.; Robinson, G. H. *Science* **2011**, *333*, 530–531.
- (172) Kong, L.; Li, Y.; Ganguly, R.; Vidovic, D.; Kinjo, R. *Angew. Chem., Int. Ed.* **2014**, *53*, 9280–9283.
- (173) Braunschweig, H.; Dewhurst, R. D.; Hammond, K.; Mies, J.; Radacki, K.; Vargas, A. *Science* **2012**, *336*, 1420–1422.
- (174) Mitoraj, M. P.; Michalak, A. *Inorg. Chem.* **2011**, *50*, 2168–2174.
- (175) Holzmann, N.; Stasch, A.; Jones, C.; Frenking, G. *Chem.—Eur. J.* **2011**, *17*, 13517–13525.
- (176) Bonyhady, S. J.; Collis, D.; Frenking, G.; Holzmann, N.; Jones, C.; Stasch, A. *Nat. Chem.* **2010**, *2*, 865–869.
- (177) Quillian, B.; Wei, P.; Wannere, C. S.; Schleyer, P. v. R.; Robinson, G. H. *J. Am. Chem. Soc.* **2009**, *131*, 3168–3169.
- (178) Linti, G.; Coban, S.; Dutta, D. *Z. Anorg. Allg. Chem.* **2004**, *630*, 319–323.
- (179) Soloveichik, G. L. *Mater. Mater.* **2007**, *2* (2), 11–14.
- (180) Derecskei-Kovacs, A.; Marynick, D. S. *Chem. Phys. Lett.* **1994**, *228*, 252–258.
- (181) Saeh, J. C.; Stanton, J. F. *J. Am. Chem. Soc.* **1997**, *119*, 7390–7391.
- (182) Lipscomb, W. N.; Marynick, D. *J. Am. Chem. Soc.* **1971**, *93*, 2322–2323.
- (183) Marynick, D. S.; Lipscomb, W. N. *Inorg. Chem.* **1972**, *11*, 820–823.
- (184) Gilliard, R. J.; Abraham, M. Y.; Wang, Y.; Wei, P.; Xie, Y.; Quillian, B.; Schaefer, H. F., III; Schleyer, P. v. R.; Robinson, G. H. *J. Am. Chem. Soc.* **2012**, *134*, 9953–9955.
- (185) Arduengo, A. J., III; Krafczyk, R.; Schmutzler, R.; Craig, H. A.; Goerlich, J. R.; Marshall, W. J.; Unverzagt, M. *Tetrahedron* **1999**, *55*, 14523–14534.
- (186) Frey, G. D.; Lavallo, V.; Donnadieu, B.; Schoeller, W. W.; Bertrand, G. *Science* **2007**, *316*, 439–441.
- (187) Ingleson, M. J.; Barrio, J. P.; Bacsá, J.; Steiner, A.; Darling, G. R.; Jones, J. T. A.; Khimyak, Y. Z.; Rosseinsky, M. J. *Angew. Chem., Int. Ed.* **2009**, *48*, 2012–2016.
- (188) Mondal, T. K.; Mathur, T.; Slawin, A. M. Z.; Woollins, J. D.; Sinha, C. *J. Organomet. Chem.* **2007**, *692*, 1472–1481.
- (189) Onak, T. P.; Landesman, H.; Williams, R. E.; Shapiro, I. *J. Phys. Chem.* **1959**, *63*, 1533–1535.
- (190) Wang, Y.; Xie, Y.; Abraham, M. Y.; Wei, P.; Schaefer, H. F., III; Schleyer, P. v. R.; Robinson, G. H. *Organometallics* **2011**, *30*, 1303–1306.